Affinity purification of NAD^+-dependent formate dehydrogenase (EC 1.2.1.2) and activity of FDH in miniature enzyme bioreactors

by

Dan Sanderson
B.Sc., University of British Columbia, 2002

A Thesis Submitted in Partial Fulfillment
of the Requirements for the Degree of

MASTER OF SCIENCE

in the Faculty of Biology

Supervisory Committee

Affinity purification of NAD^+-dependent formate dehydrogenase (EC 1.2.1.2) and activity of FDH in miniature enzyme bioreactors

by

Dan Sanderson
B.Sc., University of British Columbia, 2002

Supervisory Committee

Dr. David B. Levin, Supervisor
(Department of Biology)

Dr. Francis Y. M. Choy, Departmental Member
(Department of Biology)

Dr. John S. Taylor, Departmental Member
(Department of Biology)

Dr. Alisdair Boraston, External Examiner
(Department of Biochemistry)

Abstract

Supervisory Committee

Dr. David B. Levin, Supervisor
(Department of Biology)

Dr. Francis Y. M. Choy, Departmental Member
(Department of Biology)

Dr. John S. Taylor, Departmental Member
(Department of Biology)

Dr. Alisdair Boraston, External Examiner
(Department of Biochemistry)

Formate dehydrogenase from *Mycobacterium vaccae* (*Myc*FDH) was cloned and expressed from various plasmid constructs that incorporate hexahistidine tags onto the N- and C-termini of the protein. The most successful FDH variant, dual-tagged FDH L-S expressed from pET28a+, was batch-purified using ammonium sulphate precipitation and IMAC to achieve 96% homogeneity. A significant proportion of the expressed protein was insoluble, and the expression protocol did not respond to solubility optimization efforts. Expression of an FDH-NusA fusion variant appeared to be vulnerable to proteolytic degradation in the cell. None of the strains expressing tagged-FDH variants produced clarified lysate activity levels that were consistently as high as those from the original pUC119 vector. However, it is likely that the protein aggregation problems encountered are due to overloading of the protein production machinery or related causes, rather than to the presence of the tags themselves. A bioengineered FDH protein closely related to *Myc*FDH was also investigated. FDH GAV was immobilized in polyacrylamide gel to create gel discs or hollow cylinder mini-reactors. The apparent $K_{m(formate)}$ for this enzyme was 15.6 ± 3.6 mM in the immobilized state, and 17.2 ± 1.9 mM in aqueous solution. The activity of FDH GAV was reversibly inhibited by the presence of acrylamide monomer but was not affected by ammonium persulfate or TEMED (alone or in combination) after incubation for one minute. The activity of the immobilized enzyme system was determined to be at least partially limited by diffusion.

FDH GAV was also included in an *in vitro* analysis of the Methanol Linear Dissimilation Pathway (MLDP), a three enzyme system of NAD^+ - dependent dehydrogenases that oxidize methanol sequentially to CO_2. Horse liver alcohol dehydrogenase (EC 1.1.1.1) appeared to be the rate-limiting enzyme under the conditions used in these experiments, most likely due to its limited activity on methanol. The applicability of FDH and the MLDP to industry and bioelectronics is also considered.

Table of Contents

List of Tables

List of Figures

List of Abbreviations

6His:	hexahistidine tag
ADH:	alcohol dehydrogenase
AldDH:	aldehyde dehydrogenase
Amp:	ampicillin
APS:	ammonium persulfate
bp:	base pair
BSA:	bovine serum albumin
%C:	percent bis-acrylamide crosslinker (in polyacrylamide gel)
Cam:	chloramphenicol
Cd:	cadmium
CLEA:	cross-linked enzyme aggregate
CPIDER:	cylindrical polyacrylamide-immobilized dehydrogenase enzyme reactor
dATP:	deoxy-adenosine tri-phosphate
D_{crit}:	critical depth
ddH_2O:	distilled deionized water
DEAE:	diethylaminoethyl
DNase I:	deoxy-ribonuclease I (from bovine pancreas)
DTT:	dithiothreitol
FAD:	flavin adenine dinucleotide (oxidized)
FADH:	flavin adenine dinucleotide (reduced)
FalDH:	formaldehyde dehydrogenase
FDH:	formate dehydrogenase
FDH GAV:	bioengineered formate dehydrogenase purchased from Innotech MSU
FDH L-S:	formate dehydrogenase with a long N-terminal tag and a short C-tag
FDH X-S:	formate dehydrogenase with no N-terminal tag and a short C-terminal tag
FDH X-L:	formate dehydrogenase with no N-terminal tag and a long C-terminal tag
FDH WT:	wild type formate dehydrogenase (untagged and unmodified)
GFP:	green fluorescent protein

HFCS:	high fructose corn syrup
HLADH:	horse liver alcohol dehydrogenase
HRP:	horseradish peroxidase
IMAC:	immobilized metal affinity chromatography
IPTG:	isopropyl-β-D-1-thiogalactopyranoside
Kan:	kanamycin
Kb:	kilobase pairs
KDa:	kilodaltons
K_m:	Michaelis constant
LB:	Luria-Bertani growth medium
LDH:	lactate dehydrogenase
LeuDH:	leucine dehydrogenase
MDH:	methanol dehydrogenase
MeOH:	methanol
MLDP:	methanol linear dissimilation pathway
MW:	molecular weight
mW:	milliwatts
Myc:	*Mycobacterium vaccae* sp.
NAD^+:	nicotinamide adenine dinucleotide (oxidized)
NADH:	nicotinamide adenine dinucleotide (reduced)
Ni-NTA:	nickel-nitrilotriacetic acid
N-LS:	N-lauroylsarcosine
nm:	nanometer
NusA:	protein from *E. coli* used as soluble protein fusion partner
OD_{600}:	optical density as measured at 600 nm
PCR:	polymerase chain reaction
PMSF:	phenylmethylsulfonyl fluoride
Pse:	*Pseudomonas* sp. 101
PVDF:	polyvinylidene difluoride
RNA:	ribonucleic acid
SDS-PAGE:	sodium dodecyl sulfate polyacrylamide gel electrophoresis

%T:	percent acrylamide monomer (in polyacrylamide gel)
TBS:	Tris-buffered saline
TBST:	Tris-buffered saline with Tween-20
TEMED:	N,N,N',N'- tetramethylethylenediamine
U:	unit of enzyme activity
V_{max}:	maximum achieved velocity of an enzymatic reaction
V_{init}:	initial velocity of an enzymatic reaction
WT:	wildtype
w/v:	weight to volume ratio
w/w:	weight to weight ratio
μL:	microliter
$\tau_{1/2}$:	protein degradative half-life
ΔA_{340}	change in absorbance at 340 nm

Acknowledgments

Several people have aided me over the course of my graduate work. First and foremost, I wish to thank Dr. Levin for his continued faith in me, and for his valuable advice whenever I needed it. I must also thank David Harrison, my predecessor in this project, who showed me the ropes, and helped with many problems of a practical nature. Michael Copley, Jessica Saunders, and Supipi Kaluarachchi all provided invaluable assistance in the laboratory, particularly with the cloning effort. As well, I wish to thank members of IESVic for keeping the project on track. It was a pleasure being given the chance to contribute to such a dynamic and wide-ranging team of researchers. Thanks also go to members of the Choy lab, Sherwood lab, and the Howard / Ingham lab, notably Jo, Graeme, and Jill. Of course, half the fun of working in the Levin lab is coming in to see such wonderful people every day. Beatrixe, Carlo, Dave, Daylin, Elisa, Emilie, Simon, and Tina, you have all helped make me the researcher I am today. As the last Master's student from the Levin lab to graduate from UVic, I feel justified in saying at least this: We came. We saw. We persevered.

Dedication

I would like to dedicate this thesis to my family. Mom, Dad, Ian, and Mike: You are all amazing people and I couldn't have done it without your support. Love you always.

Chapter 1 : An overview of the industrial applications of enzymes and an introduction to formate dehydrogenase

1.1) Preamble

Enzymatic processes have been used for several thousands of years to improve the quality of human life. For example, the discovery of bread-making and beer-making processes undoubtedly had an influence on the development of many ancient societies (Braidwood *et al.*, 1953; Wessel, 1984). Originally, many researchers doubted that enzymes could catalyze reactions outside of a cellular environment, but pioneering experiments done with cell-free yeast lysates proved conclusively that fermentation is possible without living cells (Buchner, 1897). In later years, many new sources of enzymes were introduced to improve processes already in use. For example, the use of enzymes in pancreatic extracts for the bating step in leather processing represented a vast improvement over the traditional means, which relied on the enzymes present in animal dung (Tauber, 1949). From 1950 to 1970, enzyme technology expanded further as new enzymes were discovered that could improve the production of pharmaceuticals, foodstuffs, and fine chemicals. Today, enzymes are even used in the household. For example, amylases, cellulases, lipases, and proteases function as stain removers in most major laundry detergents, and the enzyme papain is still widely used as the active ingredient in meat tenderizer (Buchholz *et al.*, 2005).

Naturally, a great deal of experimentation and optimization is required to make enzymatic technologies economically feasible and competitive with similar systems that are based on inorganic catalysts. Broadly speaking, there are two approaches to

maximizing the usefulness of enzymes in practical situations. Firstly, the enzyme itself may be optimized, through direct chemical modification or manipulation of the genetic code associated with the protein of interest. Secondly, the environment of the enzyme may be altered to maximize the formation of product. This could entail design optimization of the reaction vessel, or altering reaction conditions such as temperature or pH. Different applications of the same enzyme will no doubt have different requirements, and so the system must be tailored to fit each individual process. Three examples of enzymes used in industry and technology will be considered in this study; bioreactors, biosensors, and biofuel cells.

1.2) Industrial and technological applications of enzymes: Bioreactors

A bioreactor can be defined as any vessel that contains biological molecules or cells and is used to perform chemical reactions. Bioreactors are the oldest form of biotechnology. Even before the nature of enzymes or even cells was known, humans used large microbial cultures in the form of fermenters to produce foods such as cheese and yogurt, beverages such as wine and beer, and flavouring / preservation agents such as soy sauce and vinegar. Reactors using isolated enzymes as opposed to whole cells did not appear until the 1950s, when researchers realized that many industrial-scale chemical processes could be improved by utilizing biological catalysts instead of chemical ones. For example, when the price of raw sugar climbed high enough, it became profitable to use a glucose isomerase process to convert glucose into a mixture of fructose and sucrose, which became known as high fructose corn syrup, or HFCS (Klibanov, 1983).

In fact, given the alleged contribution of HFCS to the current obesity epidemic (Bray *et al.*, 2004), this process could easily be called "dangerously inexpensive".

1.3) Industrial and technological applications of enzymes: Biosensors

A biosensor can be defined as a sensing device that uses a biological component to recognize the target species, and an electrical component to transduce the biological reaction into a measurable electrical signal (Wu and Hu, 2007). The exquisite substrate specificity of enzymes makes them useful tools for electronic sensing applications. Redox enzymes in particular have evolved around electrochemically active cofactors such as NADH and FADH, and can often be interfaced with an electrode. Glucose oxidase is especially well-suited to biosensor applications because its cofactor, FAD, is tightly bound in the active site. Proper physical orientation of the enzyme via immobilization facilitates direct electron transfer from the enzyme active site into the electrode. Biosensors based on carbon paste / gold colloid electrodes have detected concentrations of glucose as low as 10 μM (Liu and Ju, 2003). Technology based on these biosensors could one day be used to create implantable glucose monitors for diabetes sufferers. Other applications include quality control of foodstuffs, and the monitoring of environmental contaminants.

1.4) Industrial and technological applications of enzymes: Biofuel cells

Biofuel cells are conceptually similar to biosensors in that both transduce the activity of redox enzymes into an electrical current. In the case of biofuel cells, however,

that current is harnessed to do useful work. The first successful biofuel cells used whole bacterial cells instead of isolated enzymes. Using a series of microbial half-cells, Cohen (1931) was able to achieve potentials as high as 35 V (albeit with a current of only a few mA) (Cohen, 1931). Typical working voltages for a single biofuel cell tend to be less than 0.5 V due to kinetic constraints (Bullen *et al.*, 2006).

Several biofuel cells fuelled by glucose have been developed (Barrière *et al.*, 2006; Katz *et al.*, 1999; Soukharev *et al.*, 2004), but in all of these setups the glucose is oxidized only once, either to gluconic acid or D-glucono-1,5-lactone depending on the enzyme used. Subsequent reactions using other enzymes would be required to utilize all of the 24 electrons theoretically available via the complete oxidation of one molecule of glucose (Davis and Higson, 2007). Realistically speaking, such a biofuel cell would require whole microbes instead of isolated enzymes. Methanol and dihydrogen, on the other hand, are attractive fuels because they can be oxidized to completion using only a few enzymes. While the maximum theoretical cell voltage for a MeOH / O_2 biofuel cell (1.19 V) is slightly less than that for a H_2 / O_2 biofuel cell (1.23 V), methanol as a fuel is much simpler to store and transport (Palmore *et al.*, 1998). Non-enzymatic fuel cells utilizing methanol have also been developed, and although an order of magnitude higher power densities have been achieved using a metal catalyst setup, methanol biofuel cells have a simpler, membraneless design, and much lower operating temperatures. Several niche opportunities exist for methanol biofuel cells (Zhang *et al.*, 2006). Portable electronic devices such as cell phones and music players are examples of the low power applications suited to this type of technology.

Next, we shall consider several methods used in the optimization of enzyme technologies and their production. The first two topics deal with modification of the enzyme's environment, with respect to physical supports for immobilizing enzymes, and the addition of compatible enzymes for sequential or coupled reactions.

1.5) Optimization of the operational environment: Enzyme immobilization

As catalysts go, enzymes are second to none; in the presence of the appropriate enzyme, reactions that would take days or even years without catalysis are completed in milliseconds. Unfortunately, since enzymes are not required to last indefinitely in the cell (eg. ornithine decarboxylase, with $\tau_{1/2} = 5$ min) (Iwami *et al.*, 1990), many enzymes cannot maintain their capabilities for long periods, especially when exposed to the harsh chemical conditions in many bioreactors. One popular and effective way to improve the lifetime and performance of industrially useful enzymes is to immobilize them on or in a support substance. An added advantage is that immobilization on macroscopic supports allows for facile separation of the enzyme and reaction mixture for easy reuse of the catalyst. Several materials in several different formats have been adopted for enzyme immobilization, from the traditional DEAE-Sephadex beads to the more contemporary nanosilica supports and cross-linked enzyme aggregates (CLEAs) (Sheldon, 2007).

Methods for immobilizing enzymes can be divided into three basic types: The first involves binding the enzymes to an inert "carrier" substance via ionic, covalent, or Van der Waals interactions. The second involves crosslinking the enzymes themselves via linking molecules such as glutaraldehyde. The third method depends on the

formation of a matrix around the enzymes, entrapping them sterically and / or covalently (Tischer and Wedekind, 1999). An advantage of this method is that more total enzyme can be immobilized than the carrier method, and the particles are often large enough to be filtered easily. As well, immobilization can offer advantages to applications using multiple enzymes. If the product of enzyme A is the substrate for enzyme B, then co-immobilization of these two enzymes together may effectively improve the yield of product by decreasing the average diffusive distance between the various enzymes. Next, we shall consider the topic of *in vivo* and *in vitro* multienzyme systems more thoroughly.

1.6) Optimization of the operational environment: Multienzyme systems

In nature, enzymes do not operate in isolation; they are often influenced by factors in the cytosolic environment such as activators and inhibitors, which could be small molecules or macromolecules like other proteins. The process of oxidative phosphorylation gives a good example of enzymes working in concert to effect an overall transfer of electrons from various different sources onto oxygen. Each enzyme complex is a link in a chain or network; the evolution of one player no doubt hinges on the changes that occurred in the other members over evolutionary history. As well, each pathway itself has evolved in response to selection at the population level of the organism. As such, it is difficult to predict whether the genes coding for a particular enzyme pathway in one bacterium would be transferable and viable in another. Moreover, when designing an artificial enzyme system, there is no guarantee that enzymes gathered from different sources will be compatible. However, using knowledge of each enzyme's kinetic properties, some rational design is possible.

Dixon (1948) described the possibility of quantitatively characterizing the kinetics of a multi-enzyme system as "scarcely practicable". Even at such an early date, however, certain points became obvious. A "chain" type of multi-enzyme system, shown here, will

$$A \xrightarrow{E_1} B \xrightarrow{E_2} C \xrightarrow{E_3} D$$

necessarily approach a steady-state situation. That is, even though there is still flux through the system, all the enzymatic reactions have "settled down" and are occurring at the same rate (Dixon, 1951). The relative amounts of each enzyme and their rate constants will determine the steady state concentrations of the intermediate species B and C. For example, it can be imagined that if a "slow" enzyme E_1 is followed by a "fast" enzyme E_2, the intermediate produced by E_1 will on average have a short residence time and a low steady-state concentration. A similar situation will arise if E_1 and E_2 have similar rates, but the concentration of enzyme E_2 is significantly higher than that of E_1 (Dixon and Webb, 1964). This approach has been used to minimize the amount of formaldehyde present in a multienzyme methanol biofuel cell constructed by the Whitesides research group (Palmore *et al.*, 1998). If the formaldehyde concentration becomes too high, crosslinking and inactivation of the enzymes could result. The biofuel cell constructed by the Whitesides research group will serve as a starting point in this study for the purposes of considering an enzyme system for the complete oxidation of methanol to CO_2.

1.7) Case study of a methanol bioanode and the biological significance of the Methanol Linear Dissimilation Pathway (MLDP)

The Whitesides biofuel cell uses three enzymes at the anode for the oxidation of methanol. These are: alcohol dehydrogenase (ADH), aldehyde dehydrogenase (AldDH), and formate dehydrogenase (FDH). Oxygen was reduced by platinum gauze at the cathode. Each of the three dehydrogenases uses NAD^+ as a cofactor, which is known to have poor electrochemical properties. To circumvent this, this cell also included diaphorase in the anodic compartment to shuttle the electrons from the NADH produced in the reaction onto benzyl viologen, which is readily oxidized at a graphite anode (Palmore *et al.*, 1998). Below is a representation of the enzyme chain used in this setup:

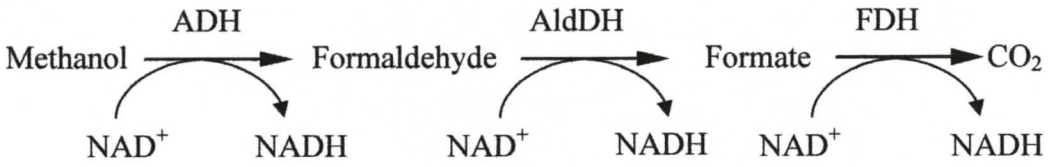

As the particular enzymes used in this cell were all from different organisms, the biological significance of this specific chain is contestable. However, several groups of organisms have enzymes that perform all of these reactions, which can collectively be called the methanol linear dissimilation pathway (MLDP). Of the chemical species in this pathway, formaldehyde and formate are both highly cytotoxic, so organisms that use methane or methanol as a carbon source (methanotrophs and methylotrophs, respectively) require enzymes that are able to consume these products quickly. In methylotrophs, formaldehyde is in fact the key branch point along the pathway from methanol to CO_2 (Yurimoto *et al.*, 2005). Figure 1.1 outlines the metabolic pathways through which

formaldehyde travels in the cell. Microbes can produce formaldehyde not only from methanol, but also from reactions involving methylated sulfur or amines and methyl halides. Formaldehyde can be consumed by a number of different pathways in methylotrophs, many of which assimilate it into three-carbon compounds. Moreover, it has been shown that multiple pathways are present and active in single species of bacteria (eg. *Burkholderia fungorum* LB400, with the capacity for formaldehyde oxidation via three of the four known routes) (Marx *et al.*, 2004).

Formaldehyde dissimilation is most quickly achieved via oxidation to formate via the enzyme formaldehyde dehydrogenase (FalDH). Usually, this requires attaching the formaldehyde to glutathione first, lowering its toxicity. Most FalDH enzymes are glutathione dependent in that they have evolved to interact with this "bound" form of formaldehyde. There are cases, however, of glutathione independent enzymes (Ando *et al.*, 1979), and these are especially interesting from the standpoint of industrial applications, as they can convert free formaldehyde into formate. Typically, once C_1 compounds have been oxidized to formate in the cell, they are either bound up into cofactors (such as N^{10}-formyltetrahydroformate, which is used in *de novo* purine synthesis) (Sheehan and Tully, 1983), or eliminated via further oxidation to CO_2. Some specialized bacteria (for example, sulfate-reducing species) are also capable of assimilating formate directly from the environment as a carbon source (Jansen *et al.*, 1984). The production of reducing equivalents from MLDP enzymes in the form of NADH is a major energy source for methylotrophs (Tishkov and Popov, 2004). In fact,

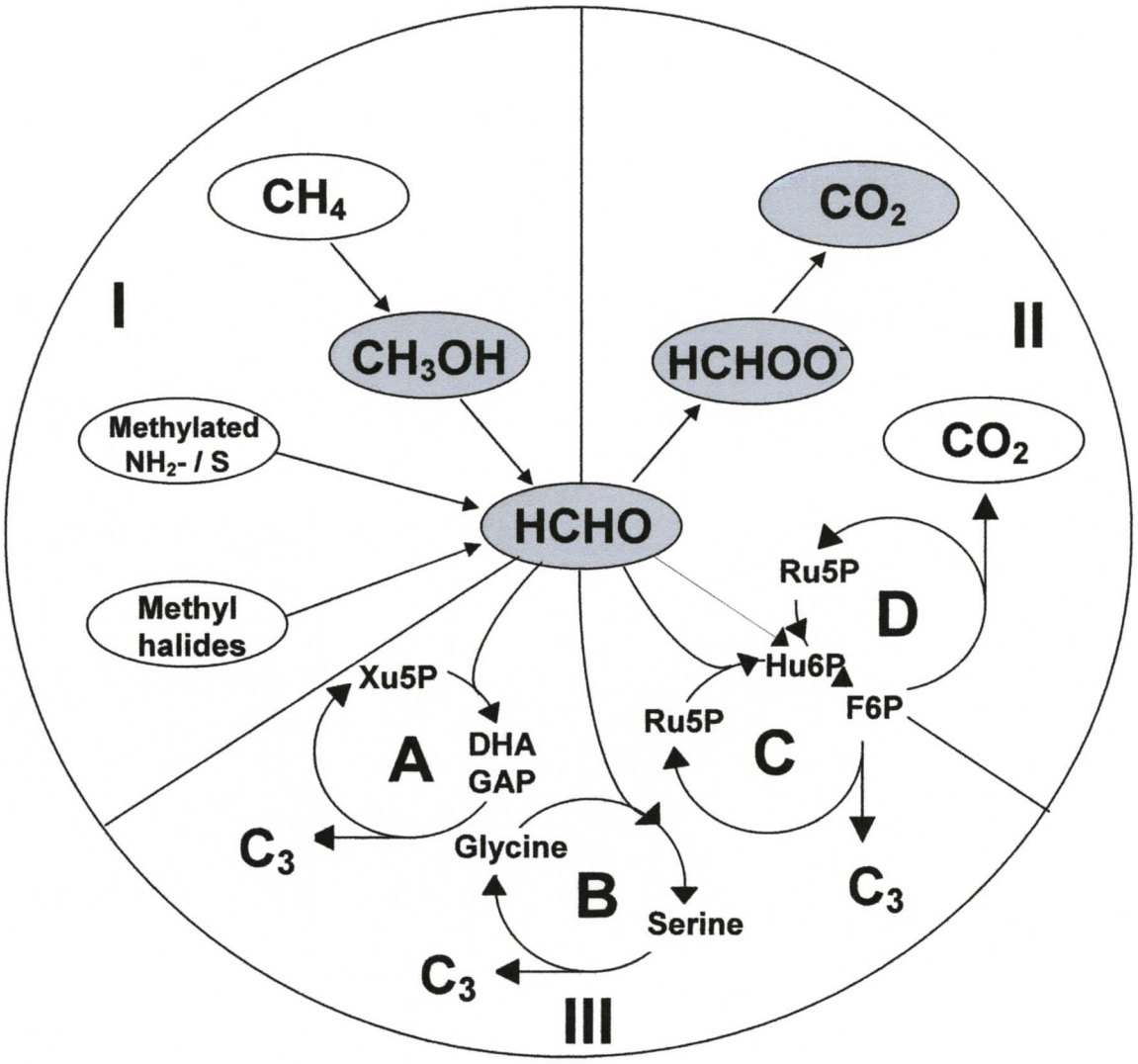

Figure 1.1 Representation of the major routes of formaldehyde formation and consumption in methylotrophic bacteria.
The methanol linear dissimilation pathway is shown in grey. **I)** Sources of HCHO generation; **II)** HCHO oxidation pathways; **III)** HCHO assimilation into C_3 compounds. **A**: Xylulose monophosphate pathway; **B**: Serine pathway; **C**: Ribulose monophosphate pathway; **D**: Cyclic oxidative ribulose monophosphate pathway. Abbreviations: Xu5P, xylulose 5-phosphate; DHA, dihydroxyacetone; GAP, glyceraldehyde 3-phosphate; Ru5P, ribulose 5-phosphate; Hu6P, D-*arabino*-3-hexulose 6-phosphate; F6P, fructose 6-phosphate). Figure adapted from Yurimoto et al., 2005.

the ability of FDH in particular to generate NADH by converting formate to CO_2 in an irreversible reaction was the major reason it was selected for use in multienzyme systems in the first place. Since the majority of redox proteins require an exogenous cofactor, which is often expensive to purchase and is consumed during the course of the reaction, bioreactors based on NADH-dependent enzymes will perform poorly if there is not a steady supply of NADH. If FDH is added to such a bioreactor, the cofactor will be alternately reduced by FDH and oxidized by the other enzyme as it is cycled between the two.

We shall now consider the bioengineering of FDH from various organisms, for the purposes of developing such a "NADH regeneration system". This is an example of the second major method for optimization of biocatalytic technologies, namely the modification of the enzymes themselves. The FDH enzyme is the major focus of the present work.

1.8) Optimization of enzymes: Background of directed evolution and bioengineering

Although the vast majority of enzymes in nature have yet to be isolated and characterized, there are a number of ways of modifying and improving known enzymes for new tasks. Rather than bioprospecting for enzymes that catalyze reactions of interest with high efficiency and stability, some researchers opt to turn unremarkable enzymes into commercially viable products using directed evolution. Directed evolution of proteins has moved beyond a simple trial and error process to advanced screening and

selection procedures that take advantage of the adaptability of the organism itself. In some cases, notably the directed evolution of enzymes that act to ligate or cleave RNA molecules, a study organism and even a starting point enzyme are not strictly necessary – an active protein can be selected from a library of partially random DNA sequences that code for only a few universally shared "scaffold" features, such as a zinc finger domain (Seelig and Szostak, 2007). Knowledge of the evolutionary history of an enzyme can sometimes give clues as to how it might be bioengineered. For example, using the knowledge that β-lactamases have naturally evolved in several cases from *D*-Ala *D*-Ala transpeptidases, researchers used a combination of random and site-directed mutagenesis to re-create this transition *in vitro* (Peimbert and Segovia, 2003). Historically speaking, however, most protein engineering research was performed with rational design in mind, based on knowledge of the protein crystal structure and the residues essential for catalysis and structural stability. The bioengineering of formate dehydrogenase is an example of this bioengineering paradigm. However, before this topic is addressed, it is necessary to present some background information on FDH.

1.9) Introduction to formate dehydrogenase

A diverse array of formate dehydrogenase enzymes can be found in nature, varying in structure, substrate specificity, and required coenzyme or cofactor. One major type, the NAD^+- dependent FDH enzymes (EC 1.2.1.2), can be found in organisms such as plants, yeast, and methylotrophic bacteria. These enzymes catalyze the reaction:

$$NAD^+ + HCOO^- \xrightarrow{FDH} NADH + CO_2$$

Like most NAD(P)- dependent dehydrogenases, a classical Rossmann fold motif is featured in the coenzyme binding domain of these proteins, and strikingly similar motifs are sometimes found in the catalytic domain also (Kutzenko *et al.*, 1998). Any FDH enzyme that is to be used in industrial processes, such as the regeneration of NADH, should be as active and robust as possible. With a specific activity of approximately 10 U/mg, the FDH from *Mycobacterium vaccae* N10 (*Myc*FDH) is among the most stable and active FDH enzymes known, making it an appealing candidate (other FDH enzymes with similar specific activities include those of *Pseudomonas* sp. 101, *Moraxella* sp. C2, and *Ancylobacter aquaticus* sp. KNK607M). By comparison, the FDH enzymes from non-microbial sources appear to be less active (ex. *Arabidopsis thaliana*, with a specific activity of 0.45 U/mg) (Tishkov and Popov, 2004).

Formate dehydrogenase from *Mycobacterium vaccae* N10 is a homodimer with 44 kDa subunits. The overall shape of the protein is an ellipsoid, with the two active sites on opposite sides. In general, the DNA sequences of NAD^+- dependent FDH enzymes are fairly conserved, but *Myc*FDH shows especially high DNA and protein sequence similarity (99% and 99.5%, respectively) with the FDH from *Pseudomonas sp.* 101 (*Pse*FDH). It is possible that many FDH genes have diverged relatively recently in evolutionary time (Galkin *et al.*, 1995). Since *Myc*FDH and *Pse*FDH are so similar in sequence and properties, much of the information gathered on *Pse*FDH can be applied with confidence to *Myc*FDH, and *vice versa*. For instance, it is probably a safe assumption that the residues essential for catalysis are identical for both enzymes, since the two amino acid differences between the two proteins are not within the active site.

1.10) Protein engineering of formate dehydrogenase

Several FDH enzymes have been subjected to protein engineering in the hopes of improving their operational lifetimes and performance in industrial applications. Thermostable and chemostable variants of *Myc*FDH have been created by site-directed mutagenesis (Galkin *et al.*, 1995; Yamamoto *et al.*, 2005), and a number of beneficial mutations have been combined to create variants of *Pse*FDH with alternate coenzyme specificity or increased activity and affinity for NAD^+ (Tishkov and Popov, 2006). The chemostable *Myc*FDH was designed to be an NADH regenerator that could withstand the harsh organic species produced in a carbonyl reductase bioreactor. To achieve this, Yamamoto *et al.* (2004) systematically replaced surface cysteine residues until a satisfactory variant was found. In the end, altering the protein in this way more than doubled the yield of the desired chemical product as compared to the unaltered version (49.9 g/L versus 19.0 g/L) (Yamamoto *et al.*, 2004). In general, NADH regeneration using FDH is advantageous because of the irreversibility of the reaction, the low cost of formate, and the fact that the product, CO_2, is inert and easily removed (Yamamoto *et al.*, 2005). The mechanism for this reaction has been best characterized for the FDH enzymes of *Pseudomonas sp.* 101 and the yeast *Candida boidinii*. From this point onward, we will refer primarily to *Pse*FDH, and, by extension, *Mycobacterium vaccae* FDH (*Myc*FDH).

1.11) Description of the FDH reaction mechanism

The *Pse*FDH reaction proceeds as a single hydride transfer, making it one of the simplest dehydrogenase mechanisms known (Tishkov and Egorov, 1985). That is, there

are no water molecules directly involved, or proton abstraction steps by amino acid residues in the active site. In order for the reaction to proceed, the NAD^+ and formate must be bound to the enzyme in a ternary complex. The binding order of formate and NAD^+ is random (Popov and Rodionov, 1978). Upon binding in the active site, the NAD^+ changes from a primarily "closed" conformation to an open formation in which the C-4 atom of the nicotinamide ring is positioned favorably for interaction with the formate. In brief, the Y-shaped formate molecule is positioned close to the nicotinamide ring, with the hydrogen (bottom part of the Y) pointing directly at the C-4 atom. This positioning minimizes steric interactions that could arise from the oxygen atoms in formate, or the hydrogen atoms in the nicotinamide (Tishkov and Egorov, 1985). Kinetic studies of this protein suggest that the substrate and coenzyme binding sites exist independently of each other and are not formed upon binding of the other substrate. However, binding of one species will increase the binding affinity for the other by 3.5 fold, presumably due to a conformational change (Popov and Lamzin, 1994).

The NAD^+ and formate access the active site via a "substrate channel" that penetrates approximately 15 Å down from the surface of each subunit (Lamzin *et al.*, 1994). After binding, the essential amino acid residues in the active site and a few key water molecules destabilize the ground state and stabilize the transition state of the reaction long enough for one bond (in formate) to break, and another to form, producing NADH and CO_2. The hydride ion transferred can be thought of as two electrons and a proton. Electrostatic effects are important in this reaction, as well as the perturbation of the carboxamide group on the nicotinamide ring (Popov and Tishkov, 2003). After the

reaction occurs, the products diffuse out of the active site, and the protein switches from the "closed" conformation to the "open" conformation that is conducive to substrate binding.

1.12) Specific examples of bioengineered FDH proteins

Formate dehydrogenase is of interest not only as a textbook example of hydride transfer, but also as an example of a protein that has been "tweaked" systematically over the course of a few decades. Initial characterization experiments showed that the maximum reaction rate and the Michaelis constants of the substrate and coenzyme do not vary over a pH range of 6 to 9 (Rodionov *et al.*, 1977). As well, in a properly reducing environment (in the presence of 2-mercaptoethanol, for example), the enzyme retains full activity for half a year, even when stored at 25°C (Egorov *et al.*, 1979). These properties and others made it an attractive candidate for industrial applications. To elucidate the role of various critical amino acids in the reaction, and possibly also improve the performance of the enzyme, Tishkov and colleagues set out to create several FDH mutants, as outlined below. In this work, we shall first and foremost consider the mutants that were found to improve the operational and thermal characteristics of the protein.

Depending on the temperature of the environment, there are various routes of inactivation for the FDH protein. Above 45°C or so, thermal inactivation dominates, but below this, oxidation of cysteine residues is the primary culprit (Popov and Egorov, 1979). Thus, improving thermal and chemical stability became a natural starting point for protein engineering. As can be seen in the wildtype protein's crystal structure, there are only two cysteine residues (Cys255 and Cys354) that are exposed on the surface of

the protein (Lamzin *et al.*, 1994). The first Cys replacement mutants created, C255S and C255M, showed a promising improvement in chemical stability (200 fold increase), but also an undesirable increase in the Michaelis constant in each case (Tishkov *et al.*, 1993). Subsequent double-replacement mutants of Cys 255 and Cys 354 with alanine and serine (respectively) showed greater than 1,000-fold enhancement of chemical stability.

A similar success story can be told for improving the thermostability of the protein. One general strategy to this end is to increase the hydrophobicity of the alpha-helices. Five serine residues were selected by researchers on the basis of their position in the protein, and various combinations of substitutions were made. Alanine proved to be the best replacement of those attempted, and it was found that the effects of these mutations were approximately additive – a four point mutant had a total of 1.5 fold thermal stabilization (Rojkova *et al.*, 1999).

In total, over 60 mutants of *Pse*FDH have been generated. The seven most attractive mutations for improving thermal stability were combined in the creation of FDH T7, which shows a thermal inactivation rate constant that is 50 times lower than that of the wild-type. The best mutations for improving thermal stability were also combined with those improving operational stability to make the mutant FDH GAV. This mutant also has two-fold higher affinity for NAD^+. Both mutants have essentially the same crystal structure as the wild-type (Tishkov and Popov, 2006). FDH GAV and FDH T7 are now produced commercially by Innotech MSU, using a purification scheme that takes advantage of the high thermal stability of the proteins. A heat precipitation step at 60°C

for 20-30 minutes removes the majority of other protein species and brings the purity to around 80%, without sacrificing enzyme activity (Popov and Tishkov, 2003). To obtain a completely homogenous preparation, further purification steps are necessary. This brings us to another example of how proteins can be modified for the optimization of enzyme technology, using modern molecular biology techniques to maximize protein production and minimize cost via abbreviated purification procedures.

1.13) Optimization of enzymes: Recombinant expression and purification

Purification of proteins using chromatography is one of the cornerstones of separations science. Affinity chromatography is based on specific interactions of target proteins with a functionalized resin. One major type of affinity chromatography is based on the tendency of certain amino acid residues to form chelates with metal ions such as nickel or cobalt (Porath *et al.*, 1975). Since its inception, immobilized metal affinity chromatography (IMAC) has been developed into one of the premier methods of protein purification (Chaga, 2001). When combined with expression systems such as the DE3 lysogen strains that overexpress proteins from strong promoters such as T7, crude lysates containing high concentrations of the protein of interest can often be purified with little investment of time. However, these techniques are not universally compatible with the vast array of proteins in nature. Overexpressing proteins in *E. coli* can result in several unpredictable outcomes. For example, normally innocuous proteins can become toxic to the cell at high concentrations, or the protein can be subjected to unexpected cleavage and degradation within the cell. As well, the protein products can aggregate into insoluble "inclusion bodies" that dominate the interior of the cell. Several cases have

been documented, and cases of complete recovery of native protein conformation are rare (Baneyx, 1999). Some strategies to increase solubility of overexpressed protein are: co-expression with a chaperone protein, expression of a soluble fusion partner such as maltose binding protein or NusA, or altering the conditions of the bacterial growth culture. Unfortunately, based largely on the idiosyncrasies of each protein, such strategies can only be approached by a trial-and-error basis.

Next, the experiments of the present work will be introduced, as they relate to the topics discussed in the previous sections. The three main themes are: i) engineering affinity tags into the FDH protein, ii) testing the behaviour of FDH in an immobilized state, and iii) testing the behaviour of FDH in the larger context of an *in vitro* methanol linear dissimilation pathway.

1.14) Cloning, purification, and expression of 6His-tagged FDH using the pET system

Surprisingly, it seems that no attempts have been made to incorporate affinity tags onto the FDH enzyme to enable simplified (possibly even one-step) purification protocols. This work will investigate the possibility of adding hexahistidine tags onto formate dehydrogenase from *Mycobacterium vaccae* N10, using the pET system. The pET system is a popular group of protein expression vectors marketed by Novagen. These vectors employ a T7 promoter in combination with a *lac* operator to enable high levels of expression under induction with IPTG. The inclusion of an exogenous "dedicated" RNA polymerase (T7 RNA polymerase) that is itself only expressed in the

presence of IPTG, helps to keep basal, or "leaky" expression of the target gene to a minimum (Studier and Moffatt, 1986). As a further measure of control, the optimum level of expression can be "tuned" in certain DE3 expression strains by varying the amount of IPTG added. Varying factors such as temperature and optical density at induction can also affect the amount of 6His protein produced. Once the tagged protein is expressed, further optimization may be necessary to ensure effective binding and elution from the affinity resin.

1.15) Immobilization of FDH enzyme using polyacrylamide

One simple method used for the immobilization of enzymes is to entrap them within a polymeric gel such as polyacrylamide. This type of gel is inexpensive, porous, and exhibits favorable mechanical properties. Several enzymes have been immobilized in polyacrylamide to enable industrial processes. For example, penicillin acylase was immobilized in a polyacrylamide electro-membrane reactor to hydrolyze penicillin. This has applications for the production of penicillin derivatives (Zadražil *et al.*, 2003).

Most often, the enzymes are entrapped in gel beads of a few hundred microns in diameter, but other methods have used gel plugs or membranes. The advantage of gel beads is that they have a high surface area to volume ratio, and can be suspended in the reaction mixture using a stirred-tank apparatus. This improves the mass transport characteristics of the system. However, with such a high surface area to volume ratio, the beads are more subject to surface erosion. Another disadvantage of suspended gel beads is that any spectrophotometric measurements of the reaction must necessarily take place

in a secondary chamber outfitted with a filter. With a small, microplate-based gel cylinder setup, we may measure the reaction rate *in situ*. Although this method is primarily suited to batch-type reactors (i.e. without continuous flow), it is advantageous in the sense that several conditions can be tested in parallel in a high-throughput manner.

1.16) FDH and the characterization of an *in vitro* methanol linear dissimilation pathway

The FDH studied in this work will by necessity use formate as its substrate and produce CO_2, as the reaction is nearly irreversible. As such, this enzyme would not be of use as the first enzyme in, for example, a system designed to sequester CO_2. However, as the final enzyme in a chain, it may provide a constant "pull" in the product direction as the C_1 compounds are irreversibly removed from the reactant pool. The FDH reaction is also the most energetically efficient step in the methanol linear dissimilation pathway leading from methanol to CO_2 (Ribbons *et al.*, 1970). To create an *in vitro* form of this pathway, it is necessary to also include one enzyme that oxidizes methanol, and one that oxidizes formaldehyde. Such an enzyme system could have energy applications in the form of a biofuel cell that operates on aqueous solutions of methanol.

The methanol biofuel cell created by the Whitesides research group in 1998 achieved power densities of 0.67 mW/cm^2 (Palmore *et al.*, 1998). Other biofuel cells have improved on this result, notably the methanol/O_2 cell utilizing alcohol dehydrogenase and aldehyde dehydrogenase immobilized in Nafion™ (a polyanionic copolymer based on perfluorosulfonic acid). This cell attained power densities as high as

1.55 mW/cm^2 (Akers *et al.*, 2004). A biofuel cell featuring all three dehydrogenase enzymes immobilized in a matrix could potentially increase performance even further. The first step is to determine which enzymes to use, and test their compatibility when in solution and when immobilized in a matrix.

It should be noted that the Whitesides cell did not use enzymes specific to methanol and formaldehyde; rather, generic alcohol dehydrogenase (ADH) and aldehyde dehydrogenase (AldDH) were used, presumably because these two enzymes are well characterized and readily available. A highly active NAD^+-dependent methanol dehydrogenase does exist and may be purified from *Bacillus methanolicus*. This enzyme, however, is highly sensitive to dilution effects. A hexahistidine tag-based expression and purification effort similar to the method employed here for FDH proved to be untenable for the production of this protein (data not shown). Ultimately, the ADH from horse liver (HLADH) was selected as the first enzyme for these multienzyme experiments, as it displays higher activity with methanol than the ADH from *Saccharomyces cerevisiae*.

We selected a glutathione-independent FalDH from *Pseudomonas putida* for the second NAD^+- dependent enzyme in the chain. Initially, this protein was included in the cloning effort also, but due to difficulties involving expression, a commercial source was found instead. For the final enzyme in the chain, FDH GAV from Innotech MSU was used.

When choosing the enzyme ratios for these tests, several factors were taken into account. In order for the performance of a biofuel cell based on this system to be

comparable to literature results, the quantities of enzymes used should be similar to those used elsewhere. The Whitesides biofuel cell was used as a starting point for this purpose. Next, the enzyme concentrations were adjusted in an attempt to minimize the amount of baseline drift due to NAD^+ already present in the commercial enzyme preparations, but at the same time maximize the rate of oxidation of substrate. On a per-subunit basis, the FDH has a turnover number that is slightly higher than that for MDH, and three times that for FalDH. The turnover numbers for the whole enzymes (the number of substrate molecules consumed per molecule of enzyme per second) are indicated in Table 1.

Table 1: Turnover numbers for dehydrogenases considered for use in the testing of an *in vitro* methanol linear dissimilation pathway (MLDP)

Enzyme Name	Substrate	Turnover rate x number of subunits (s^{-1})	Reference
Methanol Dehydrogenase	Methanol	75	(Hektor *et al.*, 2002)
Horse Liver Alcohol Dehydrogenase	Methanol	0.22	(Mani *et al.*, 1970)
Formaldehyde Dehydrogenase	Formaldehyde	14	(Ito *et al.*, 1994)
Formate Dehydrogenase	Formate	20	(Galkin *et al.*, 2001)

Based on the values indicated in Table 1, it seems that MDH is a much more attractive candidate for the multienzyme system than horse liver ADH. However, due to its instability and cost of purification, it is currently unrealistic to include it. Presumably, since MDH is highly active, cells of *B. methanolicus* would also need highly active enzymes to oxidize formaldehyde and formate. However, it seems that if cultures of these cells are subjected to a large enough pulse of methanol, the downstream enzymes cannot work fast enough to dispose of the toxic intermediates, which will eventually kill

the cells (Pluschkell and Flickinger, 2002). If a soluble and active monomeric form of the MDH protein could be bioengineered, it would be an excellent candidate for overexpression in *E. coli*. Monomeric forms of FDH have been achieved by supporting the hydrophobic patches of the protein with a reverse micelle system; conversely, a non-dissociating form of MDH might be obtained by treatment with dimethyl suberimidate (Klyachko *et al.*, 1997).

There is thought to be an ideal structure to any enzyme system, at which no enzyme is "rate-limiting" (Drozdov-Tikhomirov and Dorodnov, 1992). Under these conditions there is no bottleneck in the system, and no one enzyme is the "weakest link". In other words, raising the concentration of any two enzymes in the system would make the third one rate-limiting, until the ideal structure is restored by raising the concentration of the third enzyme by an appropriate amount. A simple method to test for ideality would be to alter the enzyme concentrations one at a time and observe if the overall rate of reaction is increased or decreased.

1.17) Objective of thesis and summary of organization

The overall objective of this thesis is to determine the usefulness of the selected dehydrogenase enzymes in creating an *in vitro* version of the MLDP pathway, for use in biofuel cell applications. The first major objective is to create a reliable supply of purified FDH from *Mycobacterium vaccae* N10, using recombinant DNA techniques, heterologous protein expression systems, and protein separation techniques such as affinity chromatography. The second objective is to determine what effects, if any,

entrapment in polyacrylamide will have on the enzymes that have been selected for study. This information will be useful for determining whether these enzymes could be used in an immobilized state in a biofuel cell or other biotechnology application. The final objective is to characterize the multienzyme system itself, by manipulation of the enzyme ratios and subsequent measurement of the initial reaction rates and the percent conversion of NAD^+ to NADH.

Chapter 2 describes the methods used to construct various 6His-tagged *Mycobacterium vaccae* FDH expression vectors and the assays used to characterize recombinant FDH activity in both aqueous and immobilized conditions. Chapter 3 describes the expression and purification of the various recombinant proteins. Chapter 4 examines the results of immobilized enzyme reactions. Chapter 5 describes the characterization of an *in vitro* methanol oxidation system in solution and immobilized in polyacrylamide. Chapter 6 provides a brief summary of the material presented in the thesis and the major conclusions that were reached.

Chapter 2 : Materials and Methods

2.1) Generating vectors for the expression of FDH

All recombinant vectors were cloned and propagated using the *E. coli* strain XL2 Blue (Stratagene, La Jolla, CA). XL2 Blue cells were also used to test expression levels of the constructs FDH L-S (pUC), FDH X-S, and FDH-WT. FDH WT plasmid DNA was kindly provided by Dr. Nobuyoshi Esaki. For the expression of FDH protein from vectors FDH L-S (pET), FDH NUS, and FDH X-L, BL21(DE3) cells, BL21 pLysS cells, and NovaBlue GigaSingles were used (Novagen EMD, VWR Canlab, Mississauga, ON). Vectors pET 28a+ and pET 44 Ek/LIC, as well as BugBuster Master Mix lysis reagent were also purchased from Novagen. Oligonucleotide primers were synthesized by Alpha DNA (Montreal, QC). The primer sequences are shown in Table 2.

Plasmid purification kits were purchased from Qiagen (Mississauga, ON), and gel purification kits were obtained from Fermentas (Glen Burnie, MD). Mouse α–His antibody (1°) was purchased from Amersham, and goat α–mouse HRP-conjugate (2°) was purchased from Invitrogen (Carlsbad, CA). Bacteriophage T4 ligase was purchased from Promega (Madison, WI). DC assay reagents were purchased from Bio-Rad (Hercules, CA). Restriction enzymes were purchased from NEB and Invitrogen, and were used under conditions matching the manufacturers' recommendations. All other reagents were purchased from Sigma-Aldrich (Oakville, ON) unless otherwise noted.

Since this study will consider the differences between versions of FDH tagged at the N-terminal and C-terminal ends, as well as the total length of heterologous protein sequence added (6His plus intervening sequence), the FDH vectors have been named in such a manner as to easily identify the form of FDH they produce. For example: FDH "L-S" represents a "long" tag at the N-terminal end, and a "short" tag at the C-terminal end. FDH "X-S" represents a form of FDH with no tag at the N-terminal end, and a short C-terminal tag.

Table 2: Primers used for the amplification of *M. vaccae* formate dehydrogenase

Primer Name[a]	Primer Sequence[b] (5' to 3')	Template in:
FDH Forward (F)	GGGAAA**CATATG**TACCGC*ATG*GCAAAGGTCCTGTG	pUC 119
FDH R1 (R)	GGGAAA**GCGGCCGC**TACCTTCTTGAACTTGGCGGCCT	pUC 119
FDH Nus (F)	GACGACGACAAGATCCGC*ATG*GCAAAGGTCCTGTG	pUC 119
FDH Nus (R)	GAGGAGAAGCCCGGTGCCTTCTTGAACTTGGCGGCCT	pUC 119
FDH R *Nco*I (R)	GGGAAA**CCATGG**TCAGCAAAAAACCCCTCAAGACCCG	pET 28a+
FDH Rp (F)	GG**GAGGAGTGCGCGTCAT**GGGCAGCAGCCATCATCATCA	pET 28a+

[a] Primer orientation is presented with F being forward and R being reverse.
[b] Restriction site sequences are shown in bold, and the FDH start codon is shown in italics.

An outline of the FDH cloning process is shown in Figure 2.1. The construction of plasmid pET28a+::FDH L-S is as follows: PCR of a 1.2 Kb amplicon containing DNA coding for all but the final amino acid of *Myc*FDH was performed using primers FDH Forward and FDH R1. The PCR reaction was started at 94°C for 2 minutes and continued for 25 cycles of 94°C, 55°C, and 72°C for one minute apiece, followed by a final seven minute incubation at 72°C for seven minutes before storage at 4°C. The amplified DNA fragment was digested with *Nde*I and *Not*I for 4 hours at 37°C. A similar digest was performed on plasmid preps of pET28a+, and the sticky ends of both gel

purified fragments were ligated together at a 1:1 molar ratio overnight at 4°C. The ligation mixture was transformed into XL2 Blue cells according to the manufacturer's instructions, and plated on LB agar plates containing 50 μg/mL ampicillin. Insertion of the intact *Myc*FDH gene was confirmed by gel electrophoresis and by nucleotide sequencing. Vector pET28a+::FDH L-S plasmid preps from XL2 Blue cells were subsequently transformed into BL21 cells and Tuner B pLysS cells for expression.

To ensure the solubility of overexpressed FDH, NusA was employed as a soluble fusion partner via the creation of plasmid pET44 Ek/LIC::FDH NUS. PCR of a 1206 bp amplicon was performed using FDH Nus F and FDH Nus R. These primers were designed to incorporate sequence appropriate for ligation independent cloning into pET44. As per the manufacturer's instructions, 0.2 pmol of PCR product were incubated in T4 DNA polymerase buffer with 2.5 mM dATP, 5 mM DTT, and 0.5 U/μL T4 DNA polymerase, in a final volume of 20 μL. This mixture was incubated at 22°C for 30 minutes in order to generate the appropriate ends for hybridization to the vector. The mixture was then heated to 75°C for 30 minutes in order to inactivate the polymerase. Within one hour of the annealing of insert to vector, the preps were transformed into NovaBlue GigaSingles Competent cells for propagation, and BL21 cells for expression, using the standard transformation protocols. Insertion of the *Myc*FDH gene was confirmed by PCR using oligonucleotide primers FDH Nus F and FDH Nus R. The hot-start PCR reaction was performed at 95°C for 2 minutes, followed by 30 cycles of: 95°C for 15 seconds, 68°C for 30 seconds, and 72°C for 90 seconds. After a final incubation at 72°C for 5 minutes, the temperature was reduced to 4°C.

Plasmids pUC 119::FDH X-S and pUC 119::FDH L-S were generated as follows: For FDH X-S, PCR was conducted using the previously constructed pET28a+::FDH L-S plasmid using primers designed to amplify the inserted *Myc*FDH gene plus the DNA coding for the C-terminal 6His tag present within the pET vector itself. For pUC::FDH L-S, the primers were designed to amplify a sequence including both the N-terminal and C-terminal tag DNA. These two fragments were digested with either *Bgl*II and *Nco*I (FDH X-S) or *Bse*RI and *Nco*I, and re-inserted into the appropriately digested pUC119::FDH WT plasmid. In other words, the original wild-type version of the *Myc*FDH gene present in pUC119 was replaced with DNA encoding the FDH protein plus either a C-terminal His tag, or both an N- and a C-terminal His tag. These vectors were used to provide a second possible expression system for 6His FDH protein. The insertions of the DNA fragments were confirmed by restriction enzyme digests and nucleotide sequencing. These plasmids were transformed into NovaBlue GigaSingles Competent cells for propagation and expression.

To ensure the C-terminal His-tag on FDH was long enough to be accessible to the affinity resin, plasmid pET44::FDH X-L was created. The FDH insert in the previously constructed pET 28a+::FDH L-S was digested out with *Nde*I and *Not*I, and ligated into a similarly digested pET44::FDH NUS vector. This removed the *Nus*A DNA along with the FDH copy already present, and created a vector coding for FDH with an "extended" C-terminal His-tag that is longer than that encoded for in pET28a+. The insertion of the new FDH fragment was confirmed by nucleotide sequencing. The FDH X-L plasmid was transformed into XL2 Blue cells for propagation, and BL21 cells for expression.

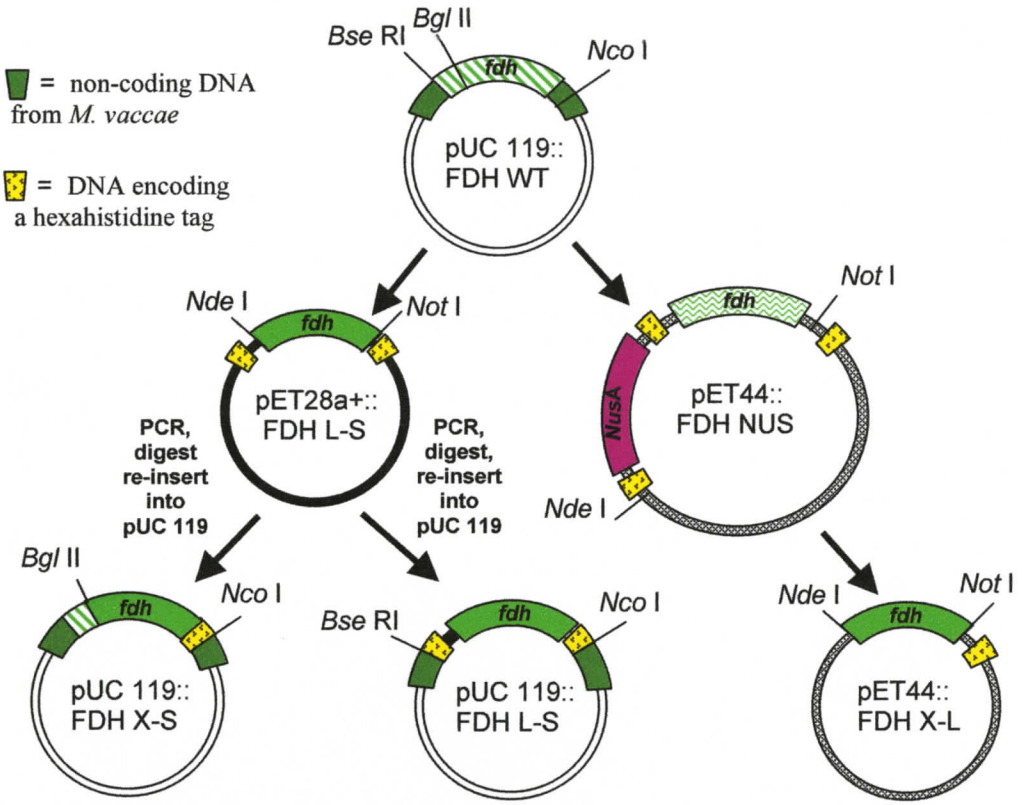

Figure 2.1 Cloning strategy for the construction of *Myc*FDH expression vectors. All pET-based vectors utilize the T7*lac* promoter, and all pUC-based vectors utilize the *lac* promoter. The DNA of the pUC vector is shown with a white ring. The DNA of pET 28a+ is shown with a black ring. The DNA of pET 44 is shown with a cross-hatched ring. Restriction sites used in cloning all versions of FDH are indicated. The FDH genes are textured to distinguish between copies of FDH from the original pUC vector, and those subcloned into pET 28a+ and pET 44. pUC 119::FDH X-S is a fusion of two FDH genes and thus has a combination of two textures. Hexahistidine tags are indicated by speckled-yellow boxes.

2.2) Expression of FDH from various constructs

Overnight cultures (10 mL) of the various FDH expression strains were grown at 37°C in LB media containing 30 μg/mL of the appropriate antibiotic (Amp, Kan, or Kan/Cam) until OD_{600} reached ~0.7-0.8. Aliquots (3 mL) of these cultures were used to inoculate 300 mL volumes of LB, which were incubated with shaking at 37°C until OD_{600} reached ~0.8-0.9. Where appropriate, IPTG was added as an inducer at OD_{600} = 0.6 - 0.8. To determine the optimal level of induction, cultures of Tuner B pLysS cells bearing plasmid pET28a+::FDH L-S were induced with six different concentrations of IPTG (0, 0.001, 0.01, 0.1, 1, and 10 mM). Cells were pelleted by centrifugation at 5000 g for 20 minutes, and pellets were subsequently lysed for 20 minutes at room temperature with 4 mL of lysis mixture for every gram of pellet weight. The lysis mixture consisted of: 5 mg/mL DNase I, 10 mM $MgCl_2$, 10% BugBuster Master Mix lysis reagent, 1% Triton X-100, 0.1% PMSF, and 0.3 mg/mL lysozyme in 0.2 M potassium phosphate buffer (pH 7.4). Crude lysates were spun at 15,000 g at 4°C to clarify the samples, and the supernatants were tested for FDH activity. Both pellets and supernatants were visualized on SDS – PAGE for analysis.

2.3) Protein assays and SDS-PAGE

Protein concentrations were determined with the BioRad DC assay using bovine serum albumin (BSA) as a standard. Spectrophotometric measurements were performed at 750 nm using a Synergy HT microplate reader (Bio-Tek). Cell lysates were mixed with Laemmli buffer, heated for 5 minutes at 90°C, and run on 12.5% polyacrylamide

gels at 50 V for 40 minutes and then 150 V for 60 minutes using a BioRad Protean III Mini-Gel system. Bio-Rad Dual Color Precision Plus was used as a protein standard.

2.4) Western blot analysis

To confirm the expression of hexahistidine-tagged FDH protein, Western blot analysis was performed using an α-His antibody. Proteins separated by SDS-PAGE were transferred onto a PVDF membrane overnight at 30 V. After a two-hour blocking step in TBS (pH 7.4) plus 5% skim milk, this membrane was incubated with a 1:5,000 dilution of mouse α–His antibody in TBST containing 0.5% Tween-20, plus 5% skim milk powder. This preparation was mixed on a Clay Adams Nutator for one hour at room temperature. Next, the membrane was incubated for another hour at room temperature in a similar TBST-skim milk solution containing a 1:20,000 dilution of a goat α-mouse HRP conjugate antibody. The membrane was washed thoroughly with TBST between steps. Finally, the membrane was incubated for five minutes in a 1:1 solution of PIERCE Supersignal West Pico luminol chemiluminescent substrate and peroxide. The chemiluminescent signal was detected on Kodak Scientific Imaging Film using a Kodak X-OMAT 2000A film processor. Hexahistidine-tagged green fluorescent protein (GFP) from *Aequorea victoria* or peptide X563 from *Clostridium perfringens* was used as a positive control for these trials.

2.5) FDH activity assays

To test the protein samples for FDH activity, 3 μL of each clarified lysate FDH sample were assayed with 0.3 M sodium formate, 0.1 M potassium phosphate buffer and

1.6 mM NAD^+ (final concentrations) in the wells of a 96-well plate. The reaction was started with the addition of the formate solution, and the increase in A_{340} was measured with a Synergy HT microplate reader. The final volume per well (~200 µL) gives a pathlength of approximately 0.5 cm (Kiianitsa *et al.*, 2003). To ensure that the signals of the activity assays were within the linear range of the spectrophotometer, a standard curve was constructed with concentrations of NADH ranging from 0.1 mM to 10 mM. Four replicates were tested for each concentration.

2.6) Batch purification of hexahistidine-tagged *Mycobacterium vaccae* FDH

FDH was purified using a two-step process, starting with an ammonium sulfate precipitation step to concentrate the FDH and remove some of the non-FDH protein species. Since different proteins will precipitate out of solution at different concentrations of ammonium sulfate, this provides a method of protein separation. First, solid ammonium sulfate was mixed into 20 mL of a 26 mg/mL clarified cell lysate until the solution was at 45% of saturation. Next, the precipitate was spun down for 30 minutes at 7,500 g, and the supernatant was removed. More ammonium sulfate was added to this fraction, until the solution reached 65% of saturation. The solution was centrifuged for 30 minutes at 10,000 g, and the supernatant removed. The FDH-bearing pellet was resuspended in 3 mL 0.2 M potassium phosphate buffer, and the remaining salt was removed by dialysis overnight in 250 mL 0.1 M phosphate buffer. All fractions were saved and subsequently tested in a microplate activity assay at 25°C using 1.6 mM NAD^+, 0.3 M sodium formate, and 0.1 M potassium phosphate buffer.

Small-scale purification of 6His-tagged *Myc*FDH using Sigma HIS-Select Nickel Affinity Gel was performed in accordance with the manufacturer's instructions. All centrifugation steps were at 5,000 g for 30 seconds, and all incubation steps were at 25°C. The resin was first equilibrated in buffer A (50 mM $NaH_2PO_4 \cdot H_2O$ at pH 8.0, 0.3 M NaCl) and then centrifuged so the buffer could be removed. Next, 100 µL of a 3.2 mg/mL *Myc*FDH solution expressed from pET28a+::FDH L-S were added and mixed by inversion for one minute in a 1.5 mL microcentrifuge tube. Protein expressed from pUC119::FDH X-S was also tested for its interaction with the HIS-Select resin. After the binding step and subsequent centrifugation, the resin was washed twice with Buffer A, and finally eluted with 50 µL of elution buffer (identical to buffer A, with the addition of 250 mM of imidazole). The samples were visualized on SDS-PAGE and selected fractions were measured on a Bio-Rad Experion Automated Electrophoresis System in order to estimate percent purity.

2.7) Testing the compatibility of FDH GAV with various components of the polyacrylamide gel

For these and all subsequent trials, FDH GAV from Innotech MSU was used in place of *Myc*FDH. To assess the effects of polyacrylamide gel on FDH GAV, inhibition assays were performed using each individual gel component; TEMED, ammonium persulfate (APS), and a 19:1 acrylamide:Bis-acrylamide mixture. Spectrophotometric FDH assays similar to those mentioned in Section 2.5 were performed with the addition of 0.05% APS, 0.1% TEMED, and a combination of both APS and TEMED. Concentrations of acrylamide ranged from 0.1% to 12.5%. To account for the possibility

that any inhibitory effects of acrylamide could be due to an increase in viscosity, similar concentrations of glycerol were used as a comparison for these tests. Finally, to test for the reversibility of any inhibition due to acrylamide, a Novagen D-tube was used to remove the acrylamide via dialysis. The solution was then re-tested in a regular (no acrylamide) activity assay.

2.8) Determining $K_{m(formate)}$ of FDH GAV in aqueous solution and entrapped in polyacrylamide

To measure the Michaelis constant (K_m) for formate of FDH GAV in solution, various concentrations of sodium formate ranging from 0.01 mM to 300 mM were used to determine the shape of the substrate-velocity curve. All tests were performed at room temperature using 0.1 M potassium phosphate buffer (pH 7.4), 1 mM NAD^+ and 0.15 U FDH GAV, in a final volume of 200 µL. Measurements were made every three seconds, and initial velocity was taken as the average slope over the first 10 data points (i.e. the first thirty seconds of the assay). Curves were fitted to the Michaelis-Menten-Henri equation with GraphPad Prism V. 4.0 using an unconstrained non-linear fit method. The default settings of the software were used; the determination of the curve was unweighted with respect to each data point.

2.9) Formation of miniature Cylindrical Polyacrylamide-Immobilized Dehydrogenase Enzyme Reactors (CPIDERs) to measure the K_m of FDH

To measure the *in situ* formation of NADH from immobilized FDH, acrylamide solutions were polymerized around the edge of each microwell in the shape of a cylinder. These preparations will subsequently be referred to as Cylindrical Polyacrylamide-

Immobilized Dehydrogenase Enzyme Reactors (CPIDERs). The formation process is shown in Figure 2.2. The gel solutions were prepared as follows. First, the APS and TEMED were added to a FDH GAV / phosphate buffer solution, and then the polymerization reaction was initiated by the addition of a 19:1 acrylamide:Bis-acrylamide solution. The reagents were added in this order to minimize potential negative effects of the acrylamide monomer. The final concentrations were 12.5% acrylamide, 0.05% ammonium persulfate, and 0.1% TEMED. The reaction was mixed thoroughly and immediately dispensed into 120 μL aliquots in each microwell, such that each microwell received 0.15 U of enzyme, identical to the solvated trials. Then, 5 mm diameter plastic rods were inserted into the center of each well before polymerization occurred, to form the cylindrical shape.

After the gel had set, the rods were removed, and the gel preparations were washed continuously for one minute with ddH_2O. Next, 100 μL of 0.2 M phosphate buffer were transferred into the center of each cylinder and allowed to sit for 2 hours at 4°C. This "soak step" allowed time for loosely associated protein to leach from the polyacrylamide matrix. The buffer from these soak steps was removed and saved for later analysis. To measure the performance of the CPIDERs, 100 μL of formate and 2 mM NAD^+ were added to the center of the cylinder to begin the reaction. Taking the volume of the gel into account, final concentrations of formate ranged from 6.7 mM to 500 mM, and the final concentration of NAD^+ was 1 mM. Data points were measured every 12 seconds over a period of one hour, and the 10 consecutive data points in each trial with the maximal average slope were taken for analysis.

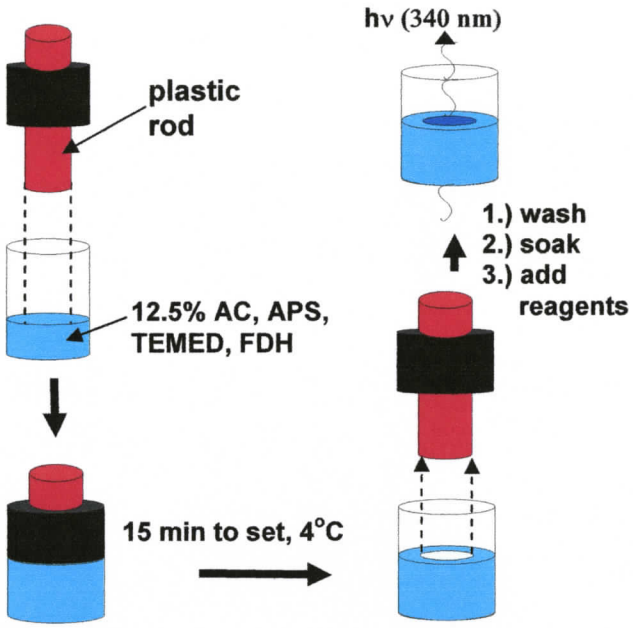

Figure 2.2 Creation of miniature enzyme reactors using polyacrylamide.
Enzyme(s), acrylamide, and polymerization catalysts are mixed in a microwell and a plastic rod is immediately inserted into the center of the well. After the gel is set, the rod is removed and the gel is washed. A two hour soak step is included to allow for enzyme leaching from the gel matrix. A mixture of NAD^+ and formate is added to initiate the reaction, and the formation of NADH is measured by monitoring the change in the absorbance of the analyte (λ= 340 nm).

2.10) Evaluating degree of enzyme leaching from polyacrylamide matrix

To account for the possibility of FDH GAV diffusing out of the polyacrylamide over the course of the assay and confounding the results, a series of tests were performed to determine the degree of enzyme leaching. First, the CPIDERs were prepared and soaked as above, but with an additional one hour soak step in phosphate buffer to simulate a test run. A 90 μL sample of analyte was then removed from each well and put into a well of a clean ½ area 96 well plate (to preserve the pathlength of the fluid). Then, 10 μL of a 10x sodium formate / NAD^+ solution was added to start the reaction. Final concentrations of sodium formate matched those used in the K_m measurements. The initial velocities of these reactions were used to calculate the baseline that would be subtracted from the K_m measurements. These calculations assumed that enzyme would accumulate in the analyte linearly over time. To test this assumption, a similar leachate test was performed with 250 mM of formate after leaching was allowed to occur for varying amounts of time.

2.11) Formation of FDH discs to measure D_{crit}

In an effort to determine an optimal polyacrylamide depth for the CPIDER system, it was necessary to vary depth, while keeping surface area and analyte volume the same. This required the creation of gel discs, with a constant concentration of FDH GAV enzyme (1.25 U/mL). These experiments were designed to measure D_{crit}, which is defined here as the thinnest gel that still gives the maximum initial activity performance. In other words, D_{crit} is the thickness beyond which diffusive limitations result in

diminished or nonexistent performance gains per unit increase of depth, over the first five minutes of the activity assay. First, gel slabs of depths ranging from 0.16 to 1.5 mm were made using a glass-plate sandwich setup, soaked in 0.2 M phosphate buffer for two hours to allow for swelling, and then cut into gel discs 2.2 cm in diameter, using sharpened metal rings. These gel discs were transferred into the well-bottoms of a Corning 12 well plate, and 3 mL of a 0.3 M sodium formate / 1 mM NAD^+ / 0.1 M phosphate buffer solution were added to measure performance. Data points were taken every 25 seconds over two hours.

2.12) Testing the MLDP enzymes in aqueous solution

To evaluate the compatibility of the three selected enzymes, they were tested in conjunction with one another in various combinations using activity assay tests similar to those mentioned in Section 2.5, using a molar ratio of 1.5:1:0.1, (HLADH : FalDH : FDH). Variations on this ratio were also tested to determine the effect of increasing or decreasing the amounts of each enzyme in the system. The initial assay concentration of NAD^+ was 1 mM, and the initial substrate concentration (methanol, formaldehyde, or formate) was 100 mM. Controls lacking one or more reaction components were set up to ensure the activity was due to the presence of one or more of the dehydrogenase enzymes.

2.13) Testing the multienzyme system immobilized in polyacrylamide

Next, using a setup and procedure identical to that used in the determination of $K_{m(formate)}$ for FDH GAV using CPIDERs (Chapter 2, Section 2.9), the effect of immobilization on the MLDP enzyme system was tested. First, the effect of immobilization was tested for each enzyme individually using its respective C_1 substrate. The no-substrate control traces were subtracted from the enzyme-substrate-NAD^+ traces to obtain a measurement of the activity of the immobilized enzymes. These assays were performed using the technique described in Section 2.9. Also, various combinations of enzymes were included in the gel setup, and activities were recorded. Initial concentrations of reactants were identical to the in-solution trials.

Chapter 3 : Expression and purification of *Mycobacterium vaccae* formate dehydrogenase

3.1) Introduction and rationale

These experiments were designed to create an FDH variant that is both highly expressed and easily purifiable, in order to have an inexpensive supply of *Myc*FDH for characterization of the MLDP system. The two main criteria for a "successful" FDH variant were defined as: i) The expressed protein must show clarified lysate specific activity levels that are consistently equal to or greater than those obtained with the wild-type protein, FDH WT; and ii) the His-tagged protein must be shown to have a significantly greater interaction with the HIS-Select affinity resin than the untagged (wild-type) protein. The FDH variants shall be considered in roughly the order in which they were created.

3.2) Methods

Construction of the various FDH expression vectors is described in Chapter 2, Section 2.1. Expression of recombinant FDH proteins, protein concentrations, SDS-PAGE, and Western Blots were conducted as described in Chapter 2, Sections 2.2, 2.3, and 2.4. Activities of recombinant FDH enzymes were determined as described in Chapter 2, Section 2.5. Purification of hexahistidine-tagged *Mycobacterium vaccae* FDH protein was conducted as described in Chapter 2, Section 2.6.

3.3) Results

3.3.1) FDH L-S

The first variant, FDH L-S, is a double-tagged variant that has an additional 24 amino acids added at the N-terminus, and 14 amino acids added at the C terminus (arbitrarily defined as a "long" and "short" tag, respectively). Each tag ended in six histidine residues. The total 38 amino acids added give it a theoretical molecular weight of 47.8 KDa, as compared to the wild-type protein, with a MW of 44.0 KDa. This difference can be seen by comparing the dominant bands in lanes 7 and 8 in Figure 3.1a. It should be noted, however, that this is a comparison between the pellet (insoluble) fraction of FDH L-S and the supernatant (soluble) fraction of FDH WT. A similar side-by-side comparison between both soluble fractions is not as immediately obvious. Indeed, the protein bands corresponding to FDH L-S were consistently much more prominent in the pellet fraction as opposed to the supernatant fraction. For both FDH WT and FDH L-S, uninduced trials consistently showed non-zero activity levels; occasionally these activities would rival those of the induced trials. As seen in Figure 3.1b, the difference in expression levels between uninduced and induced trials is much more dramatic for the insoluble fractions. In general, the activity levels of both induced and uninduced lysates of FDH L-S were much more unpredictable than those of FDH WT; while most samples had activities ranging from 20-30 mOD/min, some samples obtained with the same procedure had as high as 200-300 mOD/min. Despite numerous experiments to fine-tune the system to produce consistently high levels of expression (data not shown), the source of this variability could not be determined.

In addition to a prominent band at the expected molecular weight of FDH L-S, there are also several secondary bands in the insoluble fraction that were cross-reactive with the α-His antibody. Lysates of BL21 cells harboring pET 28a+ with no FDH insert were used as a negative control for activity trials and for visualization on SDS-PAGE. At no time did any of these trials display any FDH activity. By an unfortunate coincidence, BL21 cells appear to have a major protein band that migrates to approximately 44 KDa, somewhat obscuring SDS-PAGE visualization of proteins of this size. Ultimately, activity data supplemented with Western Analysis results were used in the evaluation of FDH variants. The inducibility of the pET system is independently confirmed in Figure 3.1b by the expression of His-tagged peptide X563 (~10 KDa). Interestingly, while the uninduced trials of FDH L-S still showed some expression, this was not seen in the uninduced trials of X563. As expected, no wild-type FDH preparations were visualized on the Western blot, as they contain no His-tags for the antibody to recognize. The results of the inducer concentration experiment are shown in Figure 3.1c. FDH L-S was expressed from Tuner pLysS cells, which contain a mutation in the Lac permease gene (LacY) to allow for homogenous entry of IPTG into all the cells in a bacterial population, making expression "tunable" with respect to inducer concentration. A wide range of inducer concentrations was chosen, but the majority of the expressed protein was insoluble regardless of the amount added. There was an overall increase in soluble expression as the amount of inducer was increased, but the difference between the lowest and highest concentration added (0.001 mM and 10 mM) was only 16 mOD/min. Interestingly, the uninduced trials showed a basal activity of 8.9 mOD/min, despite being under the tight regulatory control of the pLysS plasmid. All pellet trials were inactive.

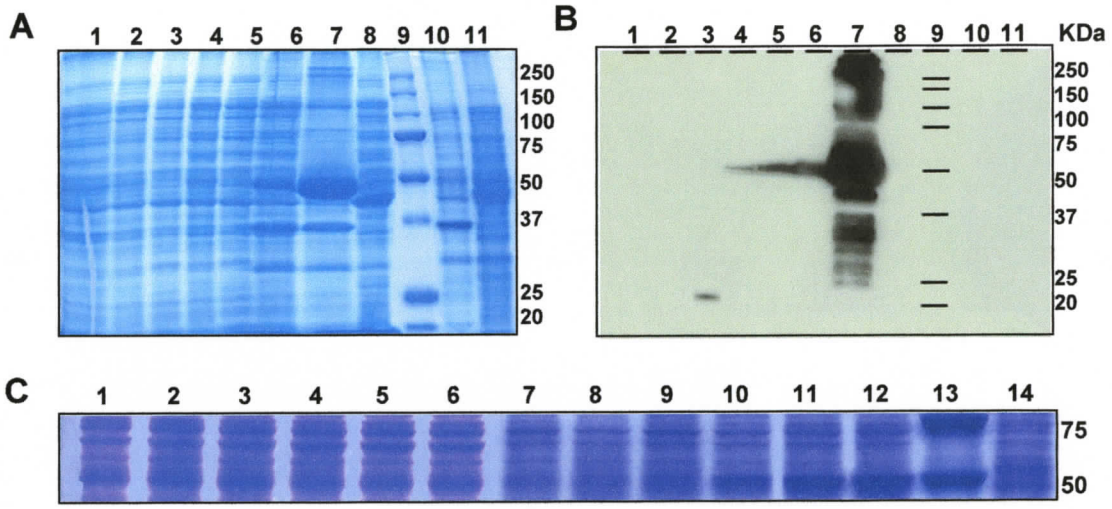

Figure 3.1 SDS-PAGE and Western analysis of FDH L-S using α–His antibody. For A) and B), the lane numbers below are identical for both the gel and Western blot. The [IPTG] for A and B was 1 mM. Lane 1: No FDH control supernatant; Lane 2: X563 "+" control, uninduced; Lane 3: X563 "+" control induced; Lane 4: FDH L-S uninduced supernatant; Lane 5: FDH L-S induced supernatant; Lane 6: FDH L-S uninduced pellet; Lane 7: FDH L-S induced pellet; Lane 8: FDH WT induced supernatant; Lane 9: Dual Color MW marker; Lane 10: No FDH ctrl pellet; 11: FDH wild-type induced pellet (expressed from pUC 119). C) Effect of varying [IPTG] on FDH L-S expression. Lane 1: Uninduced FDH supernatant; Lane 2: [IPTG]=0.001 mM supernatant; Lane 3: [IPTG]=0.01 mM supernatant; Lane 4: [IPTG]=0.1 mM supernatant; Lane 5: [IPTG]=1 mM supernatant; Lane 6: [IPTG]=10 mM supernatant; Lane 7: Uninduced FDH pellet; Lane 8: [IPTG]=0.001 mM pellet; Lane 9: [IPTG]=0.01 mM pellet; Lane 10: [IPTG]=0.1 mM pellet; Lane 11: [IPTG]=1 mM pellet; Lane 12: [IPTG]=10 mM pellet; Lane 13: Dual Color MW marker; Lane 14: No FDH control (BL21 DE3 clarified cell lysate). Both A and C are 12.5% polyacrylamide gels. 1^{o} antibody = mouse anti-His, 2^{o} antibody = goat-anti-mouse HRP conjugate.

3.3.2) FDH-Nus

Successful ligation independent cloning of the *Myc*FDH into pET44 Ek/LIC to create vector FDH-Nus was confirmed by PCR. In addition to the hexahistidine tags that are incorporated at either end of the highly-soluble NusA fusion partner, pET44 vectors also provide the option for a third tag at the C-terminal end of the protein of interest. Both options were investigated in the expression of FDH-Nus. Only trials that include the optional final tag are shown below; however, the activity levels and Western analysis results were essentially identical for both versions. Based a molecular weight calculated from the amino acid sequence of the fusion protein, one can predict that a prominent band of approximately 110 KDa should be visible in the SDS-PAGE and Western analysis results. Unfortunately, as seen in Figure 3.2a and b, no such band is visible. Notably, there is a faint band at approximately 100 KDa present in induced trials of both the soluble and insoluble fractions, which is somewhat close to the expected size. The most prominent band, however, is at about 63 KDa in both induced trials, with additional bands at 140, 42, 37, and 24 KDa. FDH L-S was used as a positive control for these trials. By comparing the intensity of the 6His-positive bands in the supernatant and pellet fractions, it appears that much of the expressed protein is again in the insoluble fraction.

3.3.3) FDH L-S expressed from pUC 119

To control for the effect of the expression system on the amount of soluble protein expressed, DNA encoding FDH L-S was transferred in-frame from pET 28a+ into pUC 119, via PCR with oligonucleotide primers that bind to pET 28a+ just outside the DNA coding for the hexahistidine tags at either end of the gene. Unique restriction sites *BseR*I

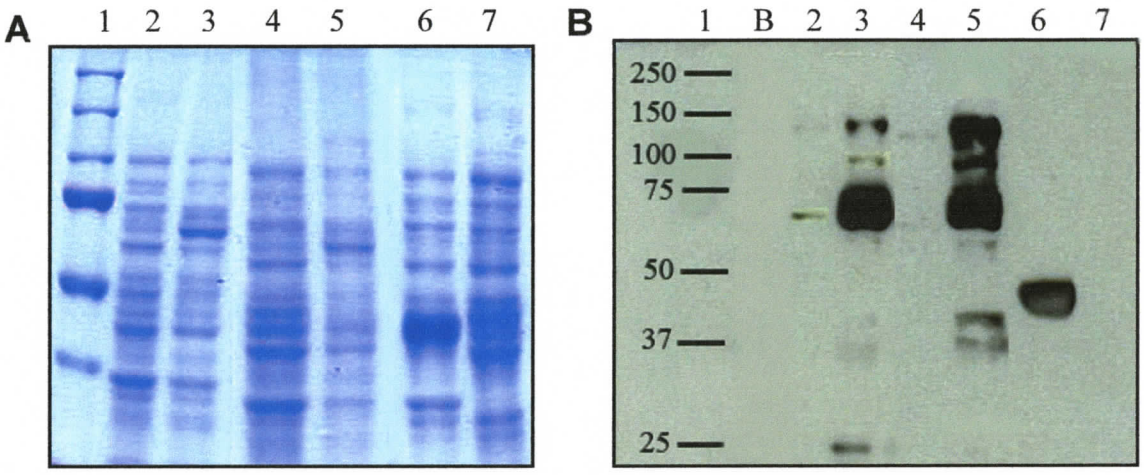

Figure 3.2 SDS-PAGE and Western analysis of FDH-Nus using α–His Antibody.
A) Coomassie stained SDS-PAGE gel. Lane 1: BioRad Dual Color MW marker; Lane 2: FDH NusA uninduced, supernatant; Lane 3: FDH NusA induced, supernatant; Lane 4: FDH NusA uninduced, pellet; Lane 5: FDH NusA induced, pellet; Lane 6: FDH L-S positive control; Lane 7: No FDH BL21 negative control. B) Western Blot. Lanes are as indicated in A). The lane labeled "B" corresponds to a blank well on the transfer gel.

and *Nco*I in the non-coding portions of mycobacterial DNA flanking the FDH WT gene were used to completely remove the untagged FDH DNA and replace it with the dual tagged version.

3.3.4) FDH X-S

To control for the possibility that some part or all of the N-terminal tag was interfering with proper protein folding, a second transfer of *Myc*FDH DNA from pET 28a+ to pUC 119 was performed, only this transfer did not include the N-terminal 6His DNA. The final construct, dubbed FDH X-S, combines the first 104 base pairs of the original FDH copy in pUC 119 with the rest of the gene (plus the C-terminal 6His) from pET28a+::FDH L-S. In this way, it is possible to express FDH protein that is tagged only at the C-terminal end. Both insertions were confirmed by nucleotide sequencing, with special attention given to ensure the His tag DNA was intact. While the FDH L-S expressed from pUC119 did not exhibit improved activity or solubility as compared to the same variant expressed from pET28a+, FDH X-S expressed from pUC119 showed activity levels that were comparable to those of the wild-type protein. There was also no evidence of the solubility problem associated with FDH L-S. However, the 6His tag on FDH L-S did not seem to be cross-reactive with α–His antibody, even under multiple test conditions, and thus could not be visualized on a Western blot. To test for the presence of the 6His tag at the protein level, FDH X-S was subjected to His-Select purification (Figure 3.3a). To re-confirm the presence of the tag at the DNA level, a restriction digest was performed on FDH X-S plasmid preparations, as shown in Figure 3.3b.

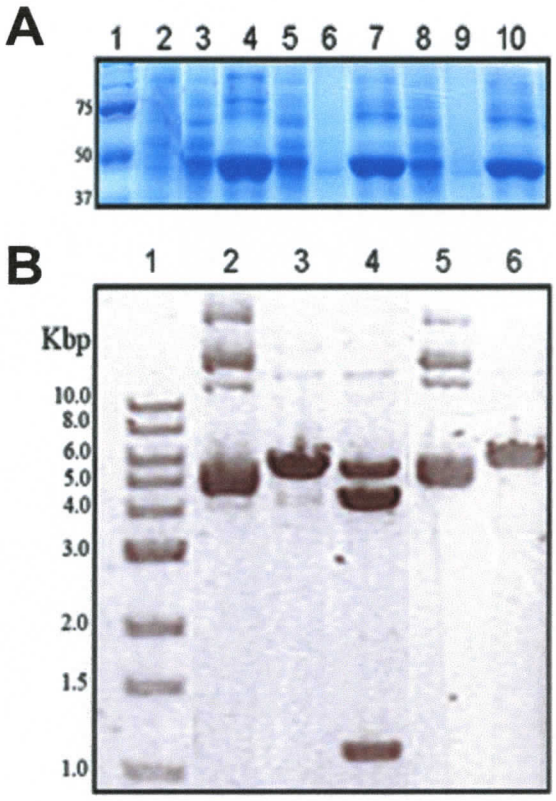

Figure 3.3 Assessment of FDH X-S C-terminal histidine tag using HIS-Select Resin and restriction enzyme digest confirmation.
A) SDS-PAGE analysis of FDH X-S. Lane 1: Dual Color MW marker (BioRad); Lane 2: No FDH control, supernatant; Lane 3: FDH wild-type, clarified lysate; Lane 4: FDH wild-type eluate from HIS-Select resin; Lane 5: FDH X-S trial 1, clarified lysate; Lane 6: FDH X-S trial 1, pellet; Lane 7: FDH X-S trial 1, eluate from resin; Lane 8: FDH X-S trial 2, clarified lysate; Lane 9: FDH X-S trial 2, pellet; Lane 10: FDH X-S trial 2, eluate from resin. B) Restriction digest confirmation of 6His vector constructs. Lane 1: NEB molecular weight marker (1 Kb); Lane 2: FDH X-S plasmid DNA, uncut; Lane 3: FDH X-S plasmid, *Not*I digest; Lane 4: FDH X-S plasmid, *Not*I and *Bgl*II digest; Lane 5: FDH WT plasmid DNA, uncut; Lane 6: FDH WT plasmid, *Not*I and *Bgl*II digest.

Two separate trials of FDH X-S were subjected to HIS-Select purification, and these results were compared with similar experiments performed on FDH WT. SDS-PAGE shows that the protein profiles of both FDH X-S eluate trials look almost identical to those of FDH WT; there are still major contaminants in all three. As well, the HIS-Select resin did not seem to be effective at binding FDH WT; more than half (59%) of the enzyme activity remained in the "unbound" fraction after incubation. When similar amounts of FDH X-S were incubated with the resin, approximately half of the enzyme activity remained in solution (47%). When the confirmed tagged FDH L-S was tested with the resin, only 33% of the FDH activity remained in solution. A more detailed treatment of FDH L-S purification shall be considered later.

The restriction enzyme digest re-confirms the nucleotide sequencing results that indicated the presence of His-tag encoding DNA. The *Not*I restriction site is directly upstream of the C-terminal 6His tag in the DNA fragment introduced from FDH L-S, and would not be present in plasmid preps containing only the original version of FDH, such as FDH WT. As well, the double digested DNA fragment is approximately 1.1 Kb, the size predicted based on a restriction map of the plasmid. So, although the His tag appears undetectable by Western Blot analysis, it is present at the DNA level.

3.3.5) FDH X-L

To control for the possibility that the C-terminal tag on FDH X-S is too short to be accessible to the HIS-Select resin, a final variant of FDH was created with an extended C-terminal hexahistidine tag. By a fortunate coincidence, the same restriction sites used

in cloning FDH into pET28a+ to create FDH L-S (*Nde*I and *Not*I) facilitate the in-frame insertion of FDH into a digested version of the FDH-Nus vector. This new vector, named FDH X-L, adds a total of 62 amino acids (including the hexahistidine tag) to the C-terminal end of the protein. Unfortunately, none of the FDH X-L trials expressed showed activity that was comparable to that of FDH WT. A summary of the specific activities for each of the FDH variants is shown in Table 3.

Table 3: Clarified lysate activities of hexahistidine-tagged *Myc*FDH variants

	FDH WT	FDH L-S	FDH L-S (pUC)	FDH-Nus	FDH X-S	FDH X-L
Activity of lysate (mOD/min)	145.8	18.4	2.3	15.0	68.9	1.5
[protein] (mg/mL)	29.6	8.0	11.4	25.2	30.6	14.0
Specific Activity (mU/mg)	96.1	44.9	3.8	11.6	43.9	2.0

Based purely on a comparison of specific activity results, the most attractive FDH variants are FDH L-S expressed from pET 28a+, and FDH X-S expressed from pUC 119. However, once the difficulties in purification of FDH X-S are taken into account, FDH L-S emerges as the most attractive candidate for purification. To concentrate the FDH for purification, ammonium sulphate precipitation was used, based on procedures used for *Pse*FDH (Egorov *et al.*, 1979). The results of this experiment and subsequent HIS-Select purification are shown in Figure 3.4 and Table 4. SDS-PAGE analysis showed that the majority of the FDH was captured in the 45-65% ammonium sulphate fraction, with little FDH remaining in solution past 65% saturation of ammonium sulphate.

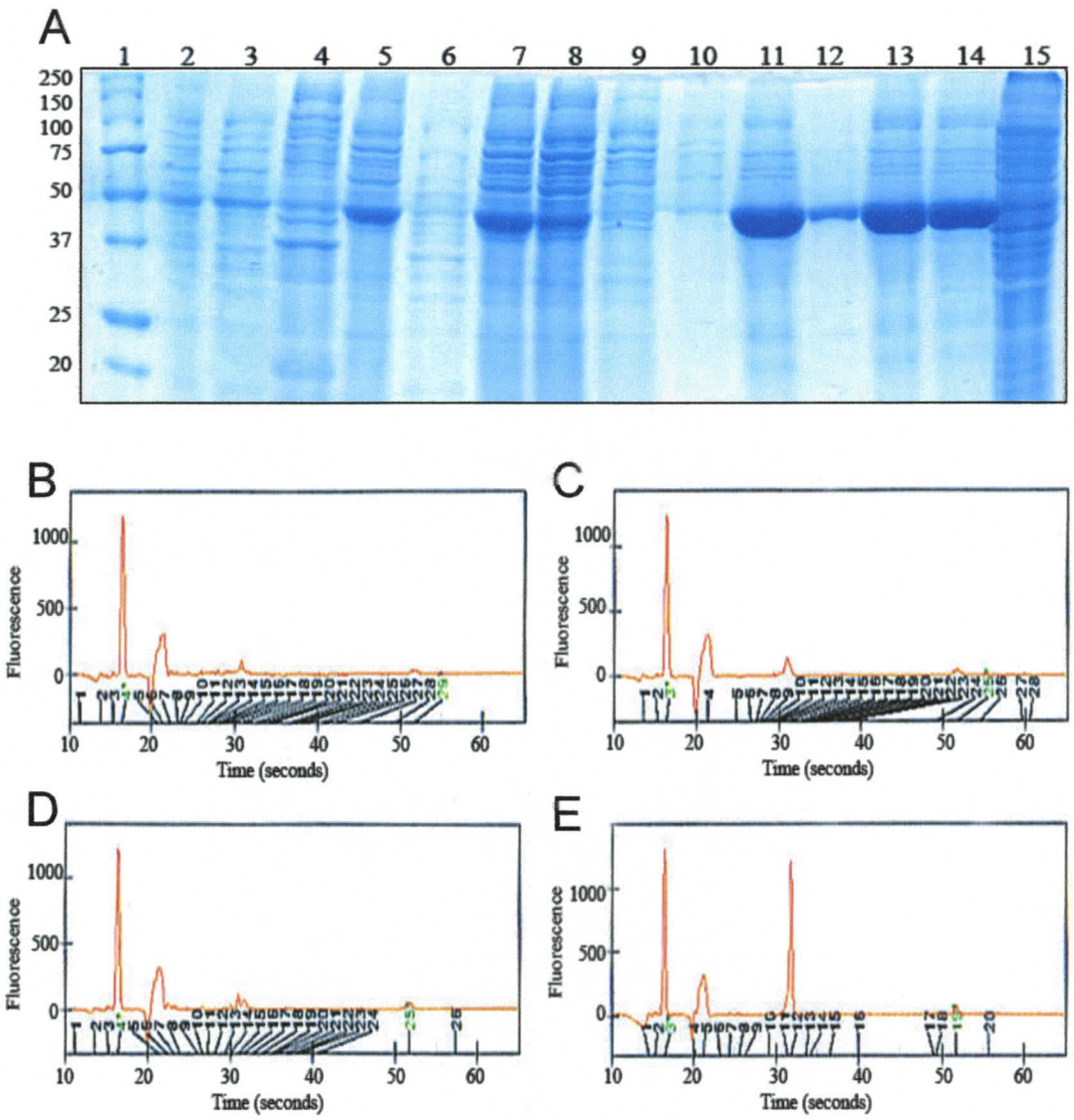

Figure 3.4 Purification of FDH L-S Using Ammonium Sulphate Precipitation (ASP) and Immobilized Metal Affinity Chromatography (IMAC).

A) Coomassie Blue stained SDS-PAGE gel. Approximately 20 µg of each sample was loaded per well of a 15% polyacrylamide gel. Lane 1: BioRad Dual Color MW marker; Lane 2: clarified FDH L-S lysate; Lane 3: 45% ASP fraction supernatant; Lane 4: 45% ASP fraction, resuspended pellet; Lane 5: 45-65% ASP fraction, resuspended pellet; Lane 6: 45-65% ASP fraction, supernatant; Lane 7: 45-65% ASP fraction, dialzyed supernatant; Lane 8: IMAC unbound fraction; Lane 9: IMAC first wash fraction; Lane 10: IMAC second wash fraction; Lane 11: IMAC first elution fraction; Lane 12: IMAC second elution fraction; Lane 13: Buffer exchanged first eluate; Lane 14: Buffer exchanged second eluate; Lane 15: No FDH control. B-E) BioRad Experion electrophoregrams used to estimate percent purity. Peaks before 22 seconds are system calibration peaks. The FDH peak can be seen at approximately 32 seconds. B) No FDH control; C) FDH WT control; D) Unpurified FDH lysate; E) IMAC first eluate.

Although a certain amount of FDH did not bind to the HIS-Select resin (Figure 3.4a, lane 8), there is a minimal amount of non-specific binding of contaminant proteins to the resin. The protein gel results suggest that the FDH eluates are nearly homogenous. This is supported by the electrophoregram results (Figure 4.3e) which show a FDH peak constituting 96% of the protein present in the sample. FDH is also the dominant peak in the pUC119 (FDH WT) and the unpurified FDH L-S lysate electrophoregrams.

Table 4: Purification summary of FDH L-S via ASP and IMAC

	Clarified lysate	45% cut snat	Resusp. 45% pellet	Resusp. 45-65% pellet	Dialyzed 45-65% pellet	>65% cut snat	HIS Select snat	Clean first eluate	Clean second eluate
Activity (mOD/ min)	234.3	103.2	2.7	309.4	363.7	4.4	100.2	296.3	60.8
[Protein] (mg/mL)	57.0	20.8	0.72	11.5	8.4	17.6	3.5	3.7	1.3
Specific Activity (U/mg)	0.08	0.096	0.073	0.52	0.84	0.049	0.56	1.56	0.91

Based on the results of Table 4, it appears that ammonium sulphate precipitation concentrates the FDH in the solution by approximately a factor of 10. The HIS-Select step removes the remaining contaminants and concentrates the sample a further factor of 2, for a total of 20-fold purification. Although the second eluate from the HIS-Select resin appears to have fewer contaminating bands, the majority of the FDH protein is in the first eluate, and so this fraction was tested using the Experion system. Buffer exchange of the eluates using diafiltration effectively prevented the FDH from

precipitating due to high salt concentrations in the elution buffer. Samples of purified FDH were stored at 4°C and at -20°C.

3.4) Discussion of cloning, expression and purification of FDH variants

3.4.1) Cloning and expression of FDH variants

Based on PCR and oligonucleotide sequencing, the sub-cloning of all five novel FDH variants was successful. However, expression experiments for each version of FDH had varying degrees of success. We shall now briefly re-consider each variant and the challenges associated with its expression.

FDH-Nus

Based on the absence of a protein band of the appropriate size, and the low activity levels obtained for FDH-Nus, it can be concluded that this variant is not being expressed in its intended form. It could be argued that the secondary bands present on the Western blot film are degradation products of FDH-Nus. It is possible that the dominant band at ~63 KDa and the fainter band at 40 KDa are degradation products of a FDH-Nus protein, with the 37 and 25 KDa bands being subsequent degradation products of the ~63 KDa band, but this conjecture does not account for the presence of the band at 140 KDa, which is clearly too large to be related to FDH-Nus.

If the expressed protein is indeed vulnerable to degradation, this may be indicative of misfolding occurring in the cell. Although *E. coli* has a host of proteases,

experiments have shown that most of the misfolded proteins are degraded by Lon and ClpYQ proteases (Missiakas *et al.*, 1996). Since BL21 cells are deficient in Lon protease, this would make ClpYQ largely responsible for degradation of any misfolded FDH-Nus. It is difficult to predict the timing of dimerization of FDH in relation to the folding process, but based on the fact that the two FDH subunits are bound together strongly via large hydrophobic regions and will not dissociate even at very high dilutions (Popov and Lamzin, 1994), it is likely a fair assumption that dimerization occurs quickly after folding, if not during folding itself. Although there are examples of dimeric proteins such as cyclomaltodextrinase being successfully expressed with a NusA fusion partner (Turner *et al.*, 2005), it seems that all else being equal, monomeric proteins would have a higher probability of attaining a properly folded conformation using this system.

FDH L-S expressed from pET and pUC vectors

In this study, FDH L-S was the only FDH variant that was both expressed at high levels and showed a strong interaction with the HIS-Select Resin. However, there were major challenges associated with reliably producing high yields of purified protein. First, the degree of variability in soluble FDH was larger between trials than between bacterial clones containing the same plasmid, despite efforts to standardize all aspects of the expression and lysis protocol. The timing of induction may have an influence; especially in cultures of FDH WT, it was found that cultures induced slightly earlier in the log phase (O.D. ~ 0.5 instead of 0.6 - 0.8) would have higher levels of expression. This effect was less obvious for cultures of FDH L-S expressed from either pET or pUC vectors. The inducibility of the FDH trials was another source of variation; although induced trials

were almost always more active than uninduced ones, the trials with no IPTG added usually had non-zero activities, and sometimes had activity levels as high as those in the IPTG trials.

The other major challenge associated with overexpressing *Myc*FDH is the solubility of the protein; by far the majority of the protein is found in the particulate, or pellet fraction. Although direct visualization of the insoluble fraction using SEM or similar techniques was not performed, it seems likely that large aggregates such as inclusion bodies are present. Surprisingly, when the pellet fraction was treated to purify the inclusion bodies from the rest of the insoluble material, it was found that chaotropes such as 8 M urea and 6 M guanidinium hydrochloride were ineffective at solubilizing the inclusion bodies. However, detergents such as Triton X-100, sodium dodecyl sulphate, and N-lauroylsarcosine (N-LS) were very effective in similar experiments. It is possible that the same hydrophobic amino acids that form the protein core and promote strong intersubunit binding are responsible for the highly insoluble nature of these protein aggregates. As a general rule, highly hydrophobic regions in proteins increase the likelihood of inclusion body formation (Mukhopadhyay, 1997).

When FDH L-S was expressed in Tuner pLysS cells with various amounts of IPTG in an attempt to optimize soluble expression, it was found that protein aggregates formed regardless of inducer concentration. As well, expression was not improved when other factors such as the duration of induction, growth temperature, and pH were altered (data not shown). Taken together, these facts suggest that the nature of FDH L-S itself,

as opposed to the pET system, is responsible for the improper folding. To be certain, the DNA encoding FDH L-S was subcloned back into pUC 119, and expressed from that vector in XL2 Blue cells. Activity levels from these trials fared even worse than when expressed from the pET vector, and so this avenue was abandoned.

It would be interesting to perform an *in vitro* denaturing-refolding experiment with homogenous preparations of FDH WT and FDH L-S to determine if FDH WT will indeed refold with higher fidelity than the tagged version. This would not be an ideal representation of the situation in the cell, however, as there are likely chaperonins and other folding modulators involved. Simple refolding experiments performed on FDH L-S aggregates solubilized with N-LS were largely unsuccessful, except in trials where cyclodextrin was included as an additive (data not shown). The fact that the N-LS must be stripped away from the protein chain with cyclodextrin suggests a strong hydrophobic interaction between the FDH and the detergent.

In the end, the main cause of protein aggregation could not be fully resolved. While it is true that the majority of the tagged variants (FDH Nus, FDH L-S, and FDH X-L) were either inactive or prone to aggregation, it is difficult to say that the tags influenced folding without an untagged control being expressed from pET 28a+. Based on the solubility patterns of a set of 27 small and medium-sized human proteins expressed with various affinity tags, Hammarström and colleagues found that an N-terminal 6His was the affinity tag most likely to render the protein insoluble (Hammarström *et al.*, 2002). It is possible that other tags may be more suitable for FDH.

FDH X-S

The only *Myc*FDH variant besides FDH L-S that showed activity levels somewhat comparable to the wild-type protein was the FDH X-S variant, expressed from pUC 119. The only difference between this protein and FDH L-S is the absence of the N-terminal hexahistidine tag. Although it is tempting to conclude that the N-terminal tag is responsible for the misfolding of the protein, it is not the only factor involved. A proper comparison would require that FDH X-S be expressed from pET 28a+ as well, since the majority of the data were obtained using this vector (although the pUC vectors are very high copy number plasmids, they are not expression vectors in the strictest sense of the word).

Another factor involved in determining the success of heterologous gene expression is the strength of the promoter associated with the gene of interest - using a strong promoter can in fact increase the likelihood of protein misfolding (Baneyx and Mujacic, 2004). In our case, the *lac* promoter in pUC is weaker than the T7 promoter in pET. This could mean that there are lower overall levels of *Myc*FDH mRNA present in cells containing the pUC vector. If this is true, it also means that the localized protein concentrations of FDH will be lower as well, since transcription and translation are coupled in prokaryotes. This could increase the likelihood of proper protein folding and limit the degree of protein aggregation. Indeed, insoluble FDH protein bands were much less obvious in the trials expressed from pUC 119.

While FDH X-S seems to have none of the solubility problems that FDH L-S does, it fails the second criterion for a "successful" variant outlined earlier; namely, it does not seem to interact with the affinity resin any more strongly than the untagged FDH. At first glance, it might seem that the C-terminal tag is simply too short or in a part of the protein that is sterically inaccessible to the Ni-NTA complex, i.e. it is a "cryptic" tag. However, this tag was not cross-reactive with α-His antibody in a denatured state either. Further complicating the matter is the fact that the presence of the 6His tag was confirmed at the DNA level. The simplest explanation for this pattern is that some post-translational processing of the FDH C-terminus is occurring in the cell. Interestingly, FDH does undergo this type of processing in *Pseudomonas sp.* 101; the final seven amino acid residues are cleaved at various points to create multiple versions of FDH that vary slightly in molecular weight and isoelectric point (Tishkov *et al.*, 1990). However, this phenomenon has not yet been documented for *Pse*FDH or *Myc*FDH expressed in *E. coli* cells. This would be a satisfying explanation for the behaviour of FDH X-S, which could be confirmed via C-terminal sequencing of the protein.

FDH X-L

It is unknown at this time why both induced and uninduced trials of FDH X-L showed only marginal amounts of enzyme activity. This particular variant was visualized only poorly on SDS-PAGE, so it is possible that "re-working" the pET 44 Ek/LIC vector by removing the *Nus*A portion has altered its expression capabilities. Using this technique, the distance between the T7 promoter / *lac* operator and the start codon was preserved, but a new start codon for FDH was introduced. Including the methionine

residue of the new start codon, a total of four new amino acids are unavoidably incorporated at the N-terminus as a result; the other three residues are a tyrosine, an arginine, and the methionine residue that was the original start codon. The DNA coding for these amino acids originated in the FDH Forward primer that was originally used to clone FDH into pET 28a+. If FDH X-L undergoes N-terminal methionine processing as the wild-type form of FDH does, this would expose the tyrosine residue that was added. According to the "N-end rule", proteins with Tyr, Arg, Lys, Phe, Leu, or Trp at the N-terminal end are rapidly targeted for termination by the cell. Proteins that have these amino acids present at the N-terminus were found to have half-lives of approximately two minutes in the cell (Tobias *et al.*, 1991). It is difficult to decide whether FDH X-L would be subject to the N-terminal methionine processing that would expose the tyrosine, however. There is some evidence that if the amino acid after methionine in the protein sequence contains a bulky side chain, (as tyrosine does) this will limit the degree of N-terminal Met processing (Hirel *et al.*, 1989). In-depth characterization of FDH X-L expression was not pursued due to its poor performance.

3.4.2) Final evaluation: Expression and purification of FDH variants

Of the FDH variants considered in this study, FDH L-S and FDH X-S showed the highest activity levels. Of these two, FDH X-S showed less variation in specific activity between trials. However, as mentioned before, the presence of the 6His tag on FDH X-S could not be confirmed at the protein level by Western Blot or by interaction with the affinity resin. This makes FDH L-S the more successful variant, based on the criteria defined in Section 3.1. Still, due to the fact that it could not consistently match the

expression levels of untagged FDH, it is a qualified success at best. The main strength of the strategy employed in this study is the short time needed for purification. Almost entirely homogenous preparations (96%) were obtainable from preparations that were concentrated with ammonium sulphate. Presumably, one step purification protocols using only the HIS-Select Resin would provide similar levels of purity, albeit at perhaps lower concentrations. This technique could be improved if it were scaled up from a batch-scale purification; if larger amounts of affinity gel were used, and elution volume minimized via column chromatography, the yield would almost certainly increase.

Most likely, scaling up the purification process would require some re-optimization of the adsorption, wash, and elution steps. One of the major disadvantages of the affinity resin is that it is not as resilient to multiple cycles as many other resins, and it must be re-charged with metal ions periodically (Knight, 1990). Another well-established method of affinity chromatography for NAD^+-dependent dehydrogenases involves using immobilized dye ligands such as Cibacron Blue to bind to the NAD^+ binding site (Subramanian, 1984). The interaction of free Cibacron Blue with *Myc*FDH was investigated, but produced no evidence of any strong binding (data not shown). All in all, it is unlikely that an affinity chromatography-based process-scale project for the purification of FDH would be able to match the cost-effectiveness of the bioengineered FDH GAV produced by Innotech MSU. There is no expensive affinity resin associated with this procedure, as it employs only a heat precipitation step followed by hydrophobic chromatography. Based on the comparatively low cost of FDH GAV (C $0.20/U as of December 2007), it was chosen as a source of FDH for subsequent experiments.

Chapter 4 : Immobilization of FDH GAV in polyacrylamide

4.1) Introduction and rationale

These experiments used FDH GAV as a model enzyme to assess the suitability of polyacrylamide as an immobilization agent for the enzymes of the MLDP. Immobilized enzymes are often stabilized or more active in an immobilized state; if this is the case for FDH GAV, it would have applications for industry and bioelectronics. It was necessary to test the effect of each individual gel component on FDH in aqueous solution. Standard activity assays were set up with the concentrations of ammonium persulfate, TEMED, and acrylamide that would be used in the formation of a 12.5% polyacrylamide gel. While the ammonium persulfate and TEMED concentrations used in these assays did not have an appreciable effect on the enzyme activity, only 36% of the FDH activity remained after incubation with 12.5% acrylamide for 1 minute. The acrylamide solution did not alter the pH of the buffered solution to any large extent, nor did any protein precipitate appear after 1 minute of incubation. However, when the acrylamide concentration was increased above 20%, the protein began to precipitate from solution.

4.2) Methods

Compatibility of FDH GAV with components of polyacrylamide gel reactants was determined as described in Chapter 2, Section 2.7. The K_m of FDH GAV in aqueous solution and immobilized in the polyacrylamide gel was determined as described in Chapter 2, Section 2.8. The construction of miniature Cylindrical Polyacrylamide-

Immobilized Dehydrogenase Enzyme Reactors (CPIDERs) to measure K_m of FDH GAV is described in Chapter 2, Section 2.9. The degree of enzyme leaching from polyacrylamide matrix was evaluated as described in Chapter 2, Section 2.10, and the formation of FDH discs to measure D_{crit} was conducted as described in Chapter 2, Section 2.11.

4.3) Results

To control for the possibility that the inhibition effect was due to an increase in viscosity from the added acrylamide, the effect of various concentrations of acrylamide were tested alongside identical concentrations of glycerol. The viscosity of glycerol is several orders of magnitude higher than that of either water or acrylamide; if any viscosity effects are present, one would expect them to be more dramatic in the presence of glycerol than in the presence of acrylamide. The results of these tests are shown in Figure 4.1a. While the addition of increasing amounts of acrylamide results in a clear decreasing trend in FDH activity, none of the glycerol concentrations have any effect. Although the inhibition by acrylamide appeared to take effect nearly instantaneously, it did not worsen with time; that is, the activity levels of the various acrylamide trials persisted over long (>1 hr) periods. To test for the reversibility of this effect, activity assays with low concentrations of acrylamide were performed using an *in situ* polymerization technique, to determine if activity would be recovered as the acrylamide monomers were used up. Unfortunately, these experiments proved logistically prohibitive. Instead, a FDH–acrylamide solution in 0.1 phosphate buffer was subjected to dialysis using a Novagen D-tube. After correcting for dilution that occurred, 96.2% of the no-acrylamide control activity was recovered.

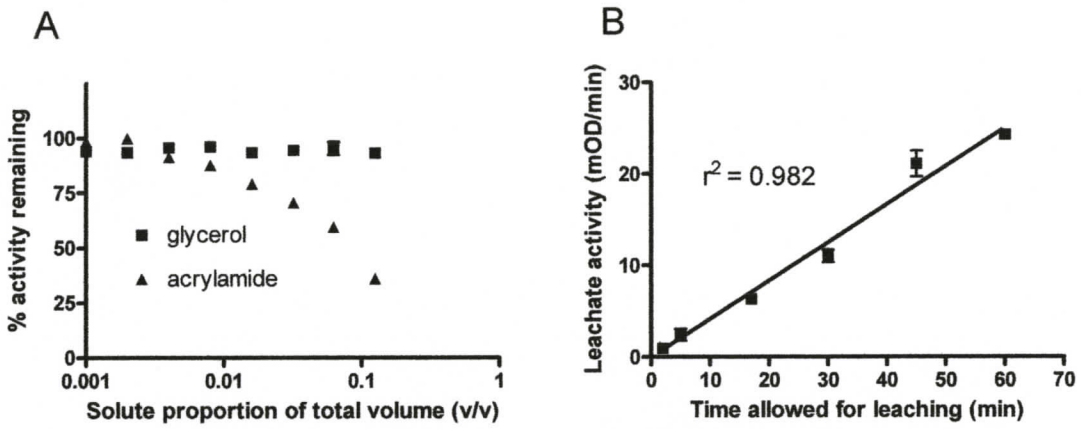

Figure 4.1 Interaction of FDH GAV with the gel matrix and gel components

A) Comparison of effects of free acrylamide monomers with that of glycerol on FDH GAV activity. B) Degree of enzyme leaching from gel over specific time periods.

In order to assess the practicality of using polyacrylamide cylinders as an immobilization scheme for FDH, it was necessary to determine the degree of enzyme leaching from the polyacrylamide matrix, and how that leaching varied over time. These results are shown in Figure 4.1b. The enzyme activity accumulating in the analyte solution increases linearly with time, at a rate of approximately 7.8 mU/min. The time range used in these tests, 0–60 minutes, was chosen because it overlaps with the time range used in the experiments to determine K_m.

A range of wall thicknesses were used in the design process of the gel cylinder enzyme reactors. Glass rods of 4, 5, and 6 mm diameter were used as molds to produce gel cylinders with walls 1.5, 1.0, and 0.5 mm thick, respectively. Ultimately, the 1.0 mm-walled cylinders were selected for testing, since the 0.5 mm cylinders were prone to infolding, and the 1.5 mm cylinders were deemed too thick for complete diffusion of substrate into the gel matrix over one hour. A sample progress curve ([formate] = 500 mM) of the gel cylinder setup is shown in Figure 4.2. The analyte absorbance follows a sigmoidal shape, not quite reaching a plateau at the end of the 60 minute assay. The maximum velocity, 68 mOD/min, is reached after approximately 1360 seconds.

The process of immobilization can often change the kinetic properties of an enzyme. To test for possible matrix interaction effects, the K_m of the FDH GAV enzyme was determined both in aqueous solution and in 12.5% polyacrylamide. In the immobilized case, the data points were taken from the area of the progress curve with the highest reaction velocity. It was found that immobilized enzyme trials using a formate

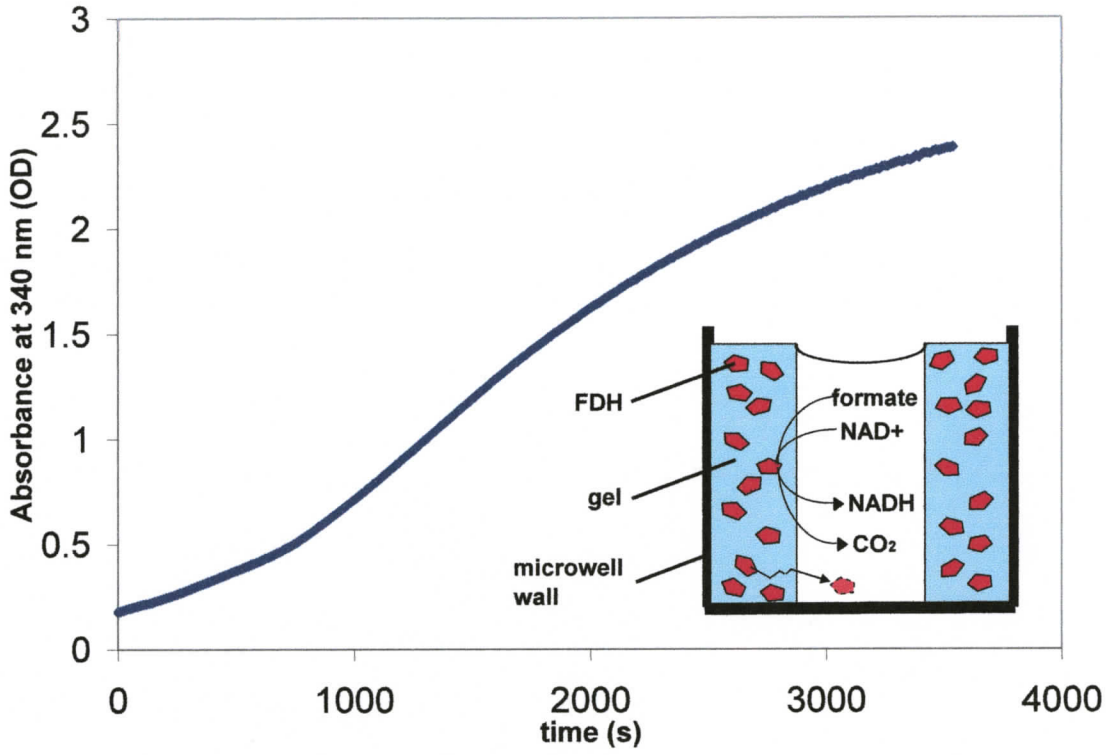

Figure 4.2 Sample progress curve of a Cylindrical Polyacrylamide-Immobilized Dehydrogenase Enzyme Reactor (CPIDER) with 500 mM formate and 1 mM NAD^+. Inset: Cutaway diagram of a CPIDER. White space indicates the analyte fluid.

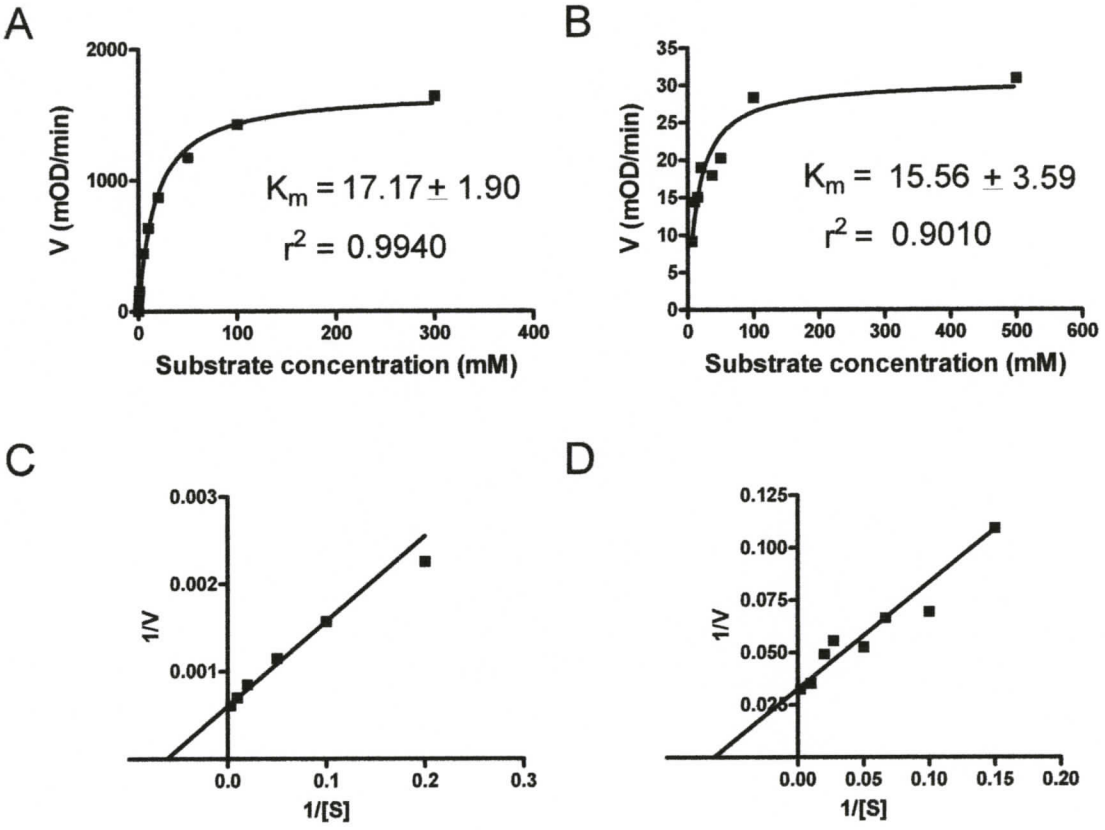

Figure 4.3 Determining K_m for solvated and immobilized preparations of FDH GAV
K_m was determined by fitting the data to the Michaelis-Menten-Henri equation using GraphPad Prism. A) Substrate-velocity data for FDH in 0.1 M phosphate buffer, [NAD^+] = 1 mM, T = 25°C; B) Substrate-velocity data for FDH immobilized in polyacrylamide (12.5% w/v T, 5% w/w C); C) Double reciprocal plot of the data points from A, using [formate] = 5-300 mM; D) Double reciprocal plot of the data points from B, using [formate] = 6.7-500 mM.

concentration lower than about 5 mM had an unacceptable signal-to-noise ratio; therefore, 6.7 mM was the lowest concentration included in this data set. Both data sets had linear double-reciprocal plots, albeit with a much higher slope in the immobilized tests, due to the lower activity levels in these trials. These data are shown in Figure 4.3.

Although there was much more variability in the replicates of the immobilized trials, both treatments gave a measurement of K_m with an r^2 value above 0.9. For the in-solution FDH, $K_m = 17.2 \pm 1.9$ mM, and the immobilized FDH had a K_m of 15.6 ± 3.6 mM. As the error ranges for these measurements completely overlap, we cannot say there is any significant difference between the two values. For the immobilized trials, measurements of background signal due to enzyme leachate were performed for each formate concentration studied. The background signal subtracted from each trial was non-trivial; on average only 82% of the measured V_{max} activities could be attributed to enzyme in the matrix. As the influence of enzyme leachate increases linearly with time, an estimate of the degree of leaching at the time-point of maximum velocity was factored into the calculation of background signal.

An important measurement in the evaluation of a matrix-based bioreactor is the amount of "dead space", that is, the amount of enzyme that is inaccessible or under-utilized in the matrix. Although it is difficult to track the movement of formate and NAD^+ into and out of the gel, we can get a sense of how the matrix dimensions influence performance by testing gel-enzyme discs of varying depths. Discs are more appropriate than cylinders in this test because they allow for the scaling of depth while keeping the

amount of surface area that is exposed to the analyte fluid constant. The data for these tests are shown in Figure 4.4. According to Figure 4.4a, it appears that matrix depth can be decreased to 0.5 mm without significantly affecting the initial reaction rate of the system. The average reaction rates are plotted versus gel depth in Figure 4.4b. Although increasing the gel depth also increases the average reaction rate, the most "efficient" gel discs on an activity per unit depth basis are the thinnest discs. In fact, gel discs of 0.17 mm were on average 4.5 times more efficient than the thickest discs of 1.5 mm. If the pattern indicated by the best-fit trendline continues, a gel disc of 0.05 mm thickness would have an efficiency of 10 times that of a 1.5 mm disc.

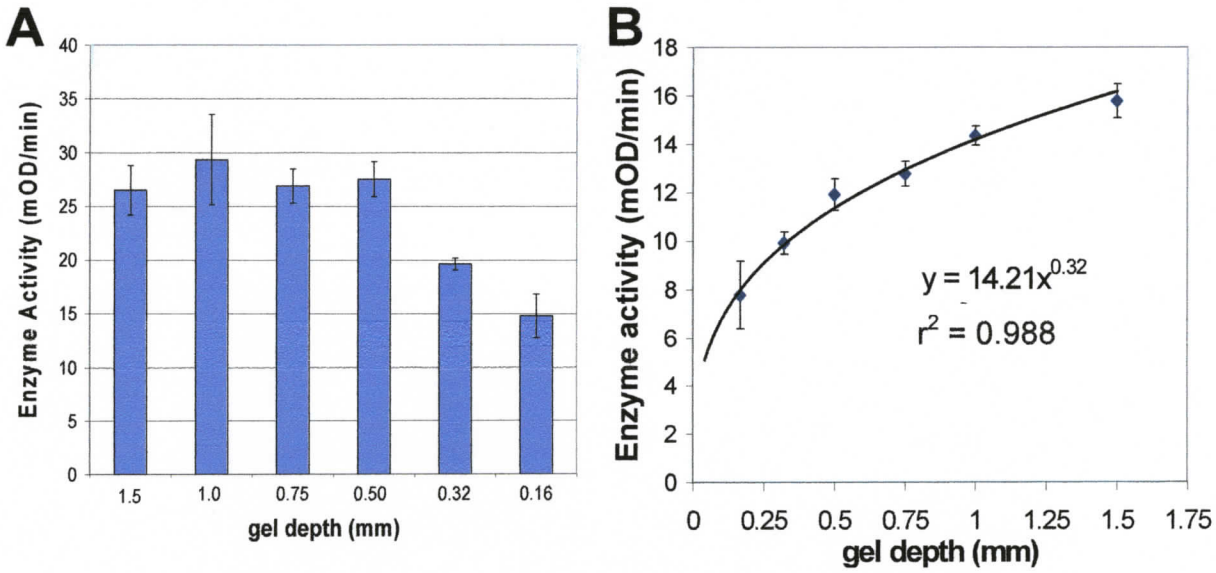

Figure 4.4 Measurement of average reaction rate and initial reaction rate for polyacrylamide discs containing immobilized formate dehydrogenase.

A) Initial reaction rate (over 5 min) of FDH gel discs, fitted to the equation $y = ax^b$.

B) Average reaction rate (over 2 h) of FDH gel discs, corrected for leachate activity.

4.4) Discussion

4.4.1) Evaluation of polyacrylamide as an immobilizing agent for FDH

After testing FDH activity in the presence of each individual gel component, it became clear that acrylamide exerted by far the largest influence. This inhibitory effect has been documented for other proteins (Mosbach and Mosbach, 1966; Nilsson *et al.*, 1972), including the formate dehydrogenase from *Candida boidinii* (Ansorge-Schumacher *et al.*, 2006). The exact nature of the interaction is unknown, but several studies have pointed to irreversible modification of certain amino acid side chains, notably Cys and Lys (Bordini *et al.*, 2000; Chiari *et al.*, 1992). Since the surface cysteines in FDH GAV have been removed through bioengineering, the essential Lys in the FDH active site is the most likely candidate with which acrylamide monomers would form an adduct. However, since i) the activity loss was not time-dependent, and ii) most of the FDH activity could be recovered via dialysis, this suggests that the acrylamide effect is non-specific and reversible for this protein. Compared with previous studies of the acrylamide effect, this study used much higher concentrations of acrylamide, and so perhaps a non-specific inhibitory effect that causes precipitation at higher (>20% w/v) concentrations is not much of a surprise. Indeed, at the concentrations of acrylamide used by Bordini and colleagues in 2000 (approximately 0.2% w/v acrylamide), there does not appear to be any inhibition of FDH GAV.

Although the reaction progress curve shown in Figure 4.2 has an obvious degree of sigmoidicity, CPIDER trials using formate concentrations less than 500 mM had a less

noticeable "lag" period, and appeared more linear. The lower the concentration of formate, the more elongated the progress curve will become, due to lower reaction rates. The exact cause of the lag period is not known, but the simplest explanation is that at the beginning of the reaction, no NAD^+ or formate has entered the gel (and no NADH has diffused out to be measured). As the substrates begin to more deeply permeate the gel, the amount of NADH released from the gel per unit time will increase. Finally, the reaction reaches a steady state situation as the curve flattens out, and the production of NADH and CO_2 decreases to nearly zero.

Besides the acrylamide inhibition effect, the other major challenge associated with these tests was the leaching of enzyme from the polyacrylamide matrix. Although the wash and soak steps minimized this effect to a certain extent, enough enzyme leached out over one hour to produce, on average, about 26% of the measured signal. However, this is ameliorated somewhat by the fact that the maximal velocity measured for the CPIDER trials was reached, on average, after about 40 minutes. Since the leaching occurs linearly with time, it can be estimated that at this point in the reaction enough leached enzyme is present to contribute an average of around 18% to the measured V_{max} values.

Pizarro *et al.* (1996) attempted to optimize the composition of polyacrylamide gel immobilized alkaline phosphatase, with the goal of maximizing activity and minimizing leachate. They found that a 31% acrylamide gel with 2% crosslinker gave optimal results (Pizarro *et al.*, 1996). Unfortunately, as seen earlier, increasing %T above around 20%

resulted in precipitation of FDH GAV. As well, decreasing the amount of crosslinker to 2% without increasing %T would likely result in an unacceptable amount of leachate being released from the gel. If total elimination of leachate were desired, it is feasible that one could pre-treat the enzymes with low concentrations of *N*-acryloxysuccinimide to create surface vinyl groups. When the acrylamide polymerization reaction occurs, these vinyl groups would be covalently cross-linked to the developing polyacrylamide matrix. This concept is based on a nanogel encapsulation technique first attempted on horseradish peroxidase (Yan *et al.*, 2006).

The K_m measurements of FDH GAV in aqueous solution (17.2 ± 1.9 mM) and in polyacrylamide (15.6 ± 3.6 mM) are in good agreement with each other and fairly good agreement with literature values. Early measurements of $K_{m(formate)}$ for *Pseudomonas sp.* 101 WT FDH gave a value of about 15 mM (Egorov *et al.*, 1979; Rodionov *et al.*, 1978); however, these results were refined in subsequent studies to approximately 7 mM (Tishkov *et al.*, 1996). The reported $K_{m(formate)}$ of FDH GAV is 7.5 ± 1.1. The discrepancy between this value and the values in this study may be partly due to limitations of the microplate reader, which is not a reaction rate analyzer *per se*; it does not facilitate rapid substrate mixing, and has an unavoidable mechanical lag of a few seconds between the addition of substrate and the start of absorbance measurements. Another possible reason for this difference is that Tishkov and colleagues used an NAD^+ concentration of 1.6 mM, versus 1 mM in this study. Using concentrations of NAD^+ much higher than 1 mM would likely put the FDH GAV reaction endpoint out of the linear absorption range of the Synergy HT.

The Lineweaver-Burk plot for the immobilized trials has a slope approximately 50 times larger than that of the aqueous trials. Thus, we can state that under these conditions, there is at least some diffusion limitation occurring (Hamilton *et al.*, 1974). However, the diffusion limitation is not severe enough to cause deviations from linearity in the Lineweaver Burk plot, so other factors may be contributing to the overall lower activities in the CPIDER trials. Some of the apparent diffusion limitation may be an artefact of the methodology used here. This technique does not truly measure *in situ* formation rates of NADH. As well, once it is formed, there will be a net diffusion of NADH in any direction that there is a concentration gradient, not only out of the gel. Therefore, the reaction rates measured are undoubtedly lower than the reality.

The similarity of the two K_m values for FDH GAV measured in this study is consistent with the notion that the polyacrylamide matrix is inert with respect to the enzyme, and does not fundamentally affect the reaction kinetics. It should be noted that this situation could change if the pH of the analyte is increased. A basic analyte would lead to hydrolysis of the pendant chains, or the "loose ends" of the polyacrylamide, forming negatively charged acrylate groups (Gonzáles-Sáiz and Pizarro, 2001). Although FDH itself maintains activity over a wide range of pH values, (pH 6-9) in this scenario much less of the negatively charged formate would enter the now polyanionic matrix.

The dimensions of an FDH molecule are approximately 11 nm by 5.5 nm by 4.5 nm (Popov and Lamzin, 1994), whereas the average pore diameter of the T= 12.5%, C=

5% polyacrylamide gels used in this study can be estimated at 33 nm (Holmes and Stellwagen, 1991). Based on these values, it seems probable that most FDH molecules will still be kinetically "free" and able to move via Brownian motion. Undoubtedly, some immobilized enzyme molecules will be inaccessible to the substrates because they are held in isolated pockets; in fact, this "trapping" phenomenon has been visualized in polyacrylamide at the level of single fluorescent molecules (Dickson *et al.*, 1996).

The results of the polyacrylamide disc experiments show that increasing the depth of the matrix above approximately 0.5 mm does not improve the initial rate of the reaction (over the first five minutes). However, the average rate of the reaction over the entire one hour time course (as well as the conversion yield of NAD^+ to NADH) improves with each subsequent increase in depth. Taken together, these two results suggest that after five minutes, some FDH is still inaccessible to formate and / or NAD^+ in discs thicker than about 0.5 mm. If five minutes were enough time for all discs to become saturated and produce a maximal response, we would expect a continuous upward trend in initial activity as depth is increased. This can be taken as further evidence that there is diffusion limitation occurring in the polyacrylamide matrix.

By analyzing each disc thickness on an activity per unit depth basis, it was determined that the thinnest discs made the most efficient use of the immobilized enzyme. One possible explanation is that enzymes immobilized closer to the gel-analyte interface are in a microenvironment that will (transiently) have the highest substrate concentration as the formate and NAD^+ enter the gel. As well, the deeper regions of the

thicker discs will act as a "product sink", preventing some NADH from exiting the gel. A rigorous mathematical analysis of the substrate / product concentration profiles in the gel would lead to a better understanding of how enzyme position in the gel affects its contribution to NADH production.

If the enzymes near the surface of the gel are indeed contributing proportionally more to the reaction, it is possible to envision a modified immobilization scheme that may improve performance. While the uniform co-immobilization technique used in this study produces a uniform distribution of enzyme, an osmotic absorption technique could concentrate the enzyme close to the gel surface. This method takes advantage of the fact that polyacrylamide can be dehydrated and rehydrated almost indefinitely. By dehydrating gel that contains no enzyme, and then rehydrating it with water containing FDH, the enzyme is drawn into the matrix osmotically. This technique was developed using ADH in polyacrylamide beads (Gorrebeeck *et al.*, 1991), and it has several potential advantages. It avoids possible inactivation effects due to acrylamide monomers, it minimizes the amount of completely isolated enzyme, and it concentrates the enzyme near the surface of the gel.

A preliminary osmotic absorption experiment was performed using dehydrated gel cylinders (N=4, wall thickness = 1 mm). Surprisingly, mean activity levels over one hour were 1.8 times higher in the co-immobilized trials than in the osmotic absorption trials. The limiting reagent in the reaction, NAD^+, was estimated to be 83% consumed by the end of the assay in the co-immobilized trials, whereas over the same time period only

an estimated 54% of the NAD^+ in the osmotic absorption trials had been converted to NADH. Using paramagnetic labeling, Gorrebeeck and colleagues determined that 15%T, 5%C gel beads will osmotically absorb ADH enzyme into approximately the first 0.25 mm of the matrix (Gorrebeeck *et al.*, 1991). Since gels of similar composition are used in this study, we might deduce that only about one quarter of the gel in the dry-swelled cylinder contains enzyme. This "dead space" may be responsible for the lower performance in the osmotic absorption trials. It remains to be seen if thinner walled gel cylinders (or perhaps gel discs) would improve performance in a similar experiment.

Regardless of the immobilization technique used, it seems that performance can be enhanced by minimizing the depth of the matrix and maximizing the amount of enzyme present. If a covalent immobilization strategy is employed, this allows the porosity of the gel to be increased in order to improve mass transfer, without risking large amounts of enzyme leachate. The immobilized enzyme itself can also be modified for the purpose of stabilizing it against the inactivating effects of acrylamide. This was attempted for the FDH from *Candida boidinii*, using random mutagenesis via error-prone PCR. Replacement of a cysteine, lysine, and a glutamate residue on the enzyme surface resulted in 4.4 fold higher residual activity after immobilization in polyacrylamide (Ansorge-Schumacher *et al.*, 2006). Conversely, the polyacrylamide matrix can be engineered to match the properties of the enzyme of interest; in the case of lipase, the hydrophobic character of the matrix was increased by co-polymerization with various methacrylates (Chauhan *et al.*, 2006).

4.4.2) Practical application of immobilized FDH

Without a doubt, the most successful application of FDH in industry is its use as an NADH regeneration system. The industrial enantioselective synthesis of lactate from pyruvate using lactate dehydrogenase provides a simple example, shown below:

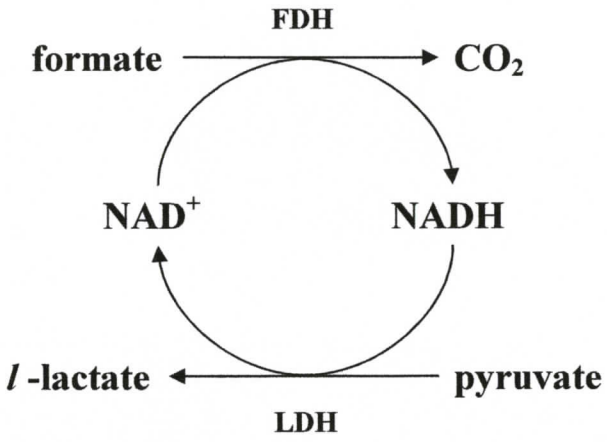

This particular system used FDH and LDH immobilized in polyacrylonitrile gel particles and resulted in the conversion of 55 grams of sodium pyruvate into lactate with a 95% yield, over a period of approximately 15 days (Shaked and Whitesides, 1980). Since LDH is also active when immobilized in polyacrylamide (Chen and Liu, 1977), this type of gel setup could be useful for an immobilized version of this system.

Perhaps the most successful NADH regeneration system using FDH is the amino acid production method developed in Germany, where the FDH reaction is coupled through its cofactor to enzymes such as leucine dehydrogenase (LeuDH) (Kragl *et al.*, 1996). This is the largest commercial process involving dehydrogenase catalysis, obtaining near 100% yields and NAD^+ cycling numbers of 35,000 to 50,000 (Ohshima *et al.*, 1985). In other words, each cofactor molecule is on average reused many thousands

of times. A gel membrane version of this LeuDH-FDH system has also been investigated, using PEG(4000) acrylate and 2-hydroxyethylacrylate crosslinked with *N,N'*-methylene (bis)acrylamide. Unfortunately, the long-term conversion ratio of α-ketoisocaproate to leucine was under 10% (Kajiwara and Maeda, 1987). Another setup of the same type using malate dehydrogenase instead of leucine dehydrogenase gave similarly disappointing results, with a maximum conversion ratio of 7.8% (Kajiwara and Maeda, 1986). It should be noted, however, that these studies used the less active yeast formate dehydrogenase. Moreover, this FDH was not bioengineered, and thus would likely be vulnerable to inactivation from the acrylate groups inherent in this type of gel. Indeed, in this study, only 14% of the in-solution FDH activity remained after immobilization. It seems that in the future, FDH GAV may find applicability in immobilization schemes where non-engineered enzymes are less chemically stable.

An interesting possibility for the improvement of FDH as a NADH regeneration system involves a main reaction in a primary chamber and the use of FDH immobilized in a gel membrane that divides a secondary reaction chamber in two. If sodium formate is added on one side of the membrane, and a salt of NAD^+ on the other, the rate at which these substrates enter the membrane could be enhanced if a current is applied across the gel membrane. This type of augmentation of mass transfer effects has been successfully utilized with penicillin G acylase immobilized in polyacrylamide (Zadražil *et al.*, 2003). The negative formate ion would be carried into the gel towards the anode, and the positive NAD^+ would be carried towards the cathode. When these two species meet FDH, they would become neutral. If a pump is also included to introduce flow into the

system, a continuous source of NADH could be produced, and cycled back to the primary reaction chamber. For this type of setup, ideally the FDH would be covalently attached to the matrix to prevent electrophoretic mobility of the protein.

Although the present study did not investigate the stability and reusability of FDH immobilized in polyacrylamide, related studies on FDH from *Pseudomonas sp.* 101 immobilized in activated glyoxal-agarose suggest that immobilized FDH may have increased stability against changes in temperature and pH, as well as the presence of organic solvents. When *Pse*FDH was immobilized in the glyoxal agarose matrix, it retained 50% of its activity (Bolivar *et al.*, 2006a). The aldehyde functionality on the glyoxal reacts with certain side chains of the protein; this is another method of covalently attaching the protein to the matrix, which often results in increased stability. A similar study was performed on ADH from horse liver, which resulted in 90% retention of enzymatic activity upon immobilization (Bolivar *et al.*, 2006b). Thus, glyoxal agarose may be an attractive alternative to polyacrylamide if covalent attachment to the matrix is desired. However, polyacrylamide is still an attractive and useful matrix for immobilization due to its low cost, resiliency, flexibility in pore size, relatively inert chemical nature, and its ease of construction.

Chapter 5 : Characterization of an *in vitro* methanol oxidation system in aqueous solution and immobilized in polyacrylamide

5.1) Introduction and rationale

The MLDP system of ADH, AldDH, and yeast FDH has been shown to function effectively in a biofuel cell setup (Palmore *et al.*, 1998), but the behaviour of the system itself was not analyzed. In all likelihood, optimization of the enzyme ratios would greatly improve the reaction rate and fuel utilization of any practical application of the MLDP, be it biofuel cell or NADH regeneration system. As a further improvement on the previous study, two enzymes with more attractive kinetic parameters (FalDH and FDH GAV) have been selected to replace AldDH and yeast FDH. The first step is to confirm that the selected enzymes are compatible with one another. That is, each enzyme must show a measurable contribution to the overall production of NADH. To accomplish this, the enzymes will be added sequentially after each previous reaction has reached steady state. For a comparison, tests will also be performed with ADH and FalDH, or all three enzymes present at the beginning of the reaction. The results of these tests may indicate which spatial arrangement of the enzymes would be most efficient at oxidizing fuel in practical applications. Previous modeling studies for the MLDP indicate that an enzyme reaction chamber containing all three enzymes utilizes fuel more completely than a series of separate chambers for each enzyme in the chain (Kjeang *et al.*, 2006). Also, by altering the amount of each enzyme used, and recording the initial activity and NAD^+ utilization, it is possible to determine which enzyme is "limiting" under the conditions used in this assay.

The methanol / O_2 biofuel cell constructed by the Whitesides research group could possibly be improved if the enzymes were immobilized in a matrix. This would serve to increase the local concentration of enzyme and perhaps augment the oxidation of methanol into CO_2. This type of enzyme coupling due to proximity is well-known in nature. For example, the majority of the enzymes of the electron transport chain are localized to one place; the mitochondrial membrane (Mitchell, 1979). There are a few examples in the literature of multienzyme systems immobilized in polyacrylamide. Notably, the activity of a three enzyme system featuring malate dehydrogenase (MalDH), citrate synthase, and lactate dehydrogenase (LDH), was found to be as much as five times more active in the immobilized state than in the free state (Srere *et al.*, 1973). This system is shown below.

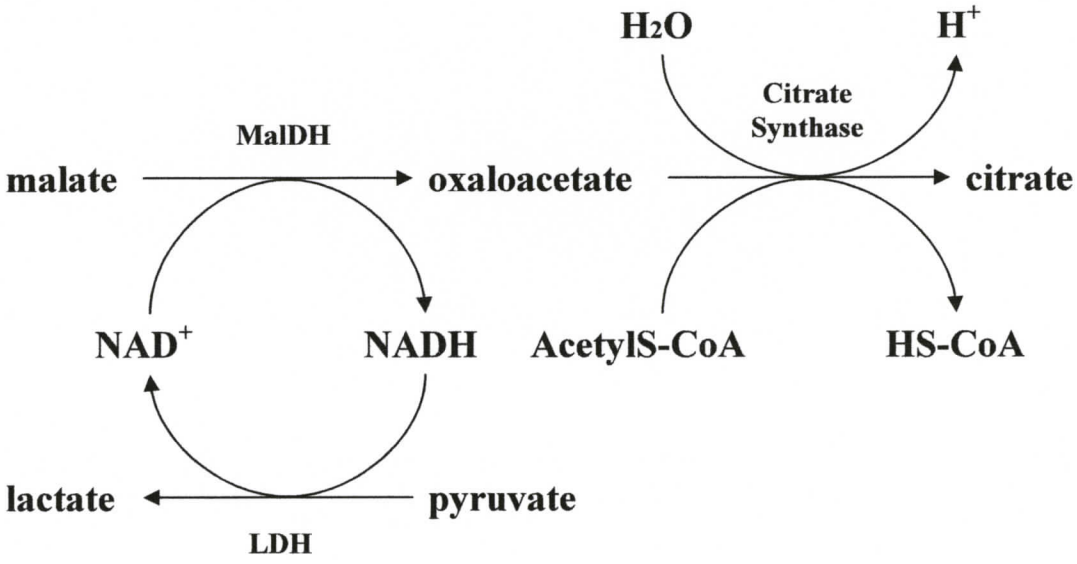

It should be noted, however, that these results were obtained from homogenized gel-enzyme particles that were suspended in a stirred-tank reactor, and are not directly comparable to our gel-cylinder setup. The setup used in the present study relies on diffusion through bulk gel, and although the overall formation of NADH occurs much

more slowly, immobilized FDH GAV trials reached reaction endpoints similar to those obtained in the aqueous solution trials. To expand on these positive results, polyacrylamide will be tested as an immobilization agent for the other two enzymes of the MLDP.

If we are to compare two or more different treatments for the oxidation of methanol using the MLDP enzymes, it is useful to know what the theoretical endpoint of the reaction will be. Since the limiting reagent is NAD^+, then if the reaction goes to completion, the final concentration of NADH should be identical to the initial concentration of NAD^+. It is necessary to ensure this final concentration of NADH is within the linear range of the spectrophotometer. To this end, a standard curve of absorbance versus NADH concentration was created.

5.2) Methods

The method used for the characterization of the in vitro MLDP system is described in Chapter 2, Section 2.12. The determination of the activity of the immobilized dehydrogenase enzymes using the gel cylinder setup is described in Section 2.9 and 2.13. The creation of the NADH standard curve is detailed in Section 2.5.

5.3) Results

The NADH standard curve is shown in Figure 5.1. The absorbance varies linearly with NADH concentrations below approximately 1.5 mM. Above this value, further

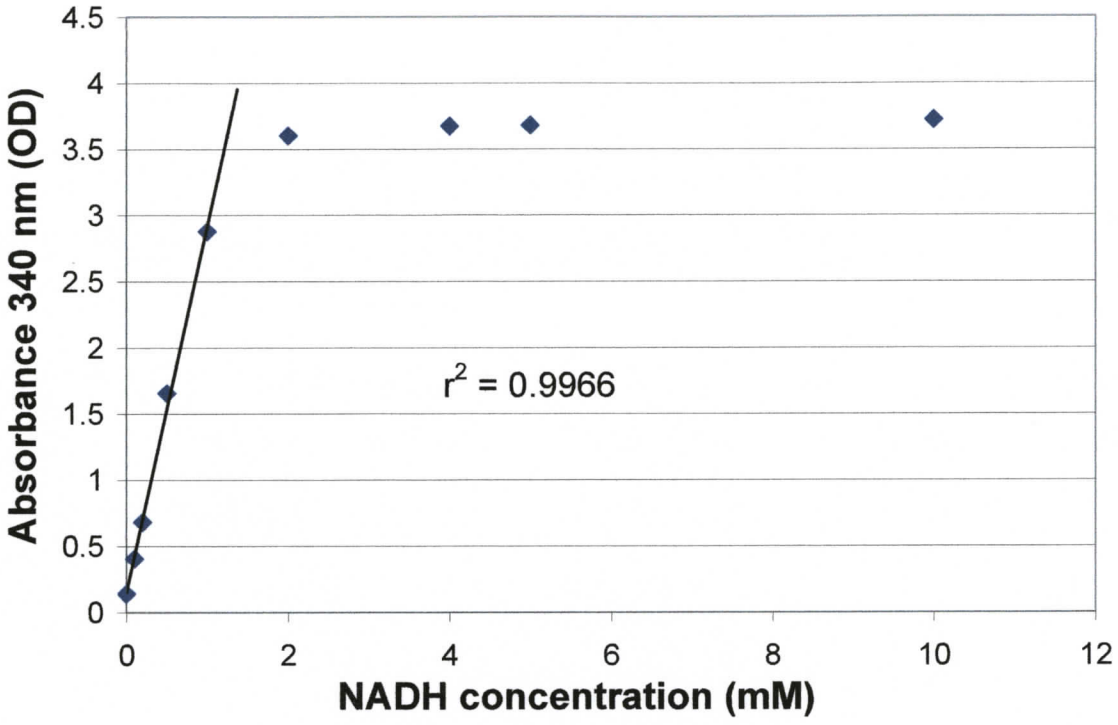

Figure 5.1 NADH standard curve for BioTek Synergy HT microplate reader. The r^2 value is given for the line following the first five data points. (N= 4 replicates)

increases can no longer be measured accurately. Based on this information and the concentrations used in the fuel cell constructed by the Whitesides research group, an initial NAD^+ concentration of 1 mM was selected for the characterization of this multienzyme system. Using the standard curve, complete utilization of the NAD^+ would give a final absorbance $A_{340} = 2.88$. Subtracting the background absorbance gives a value of 2.74. This value was used to calculate what proportion of NAD^+ was converted to NADH, which will be referred to as the degree of NAD^+ utilization.

The results for the simultaneous and stepwise oxidation of methanol using dehydrogenase enzymes are shown in Figure 5.2. Adding FalDH after the ADH reaction reached steady state induced a second progress curve; the subsequent addition of FDH to these trials also augmented the reaction when it was added next, but not as dramatically as the addition of FalDH. It was also found that trials containing all three enzymes from the start of the reaction reached a higher endpoint than the trials in which enzymes were added stepwise. Again, the addition of both FalDH and FDH each had a positive effect on both the initial rate and the total utilization of NAD^+. FalDH did not have any effect on the change in absorbance for trials with 0.1 M methanol unless ADH was also present, and FDH required both ADH and FalDH to be present to have an effect in the methanol trials. A small increase in absorption was measured for the no NAD^+ control and the no substrate control, but the initial velocities of trials with both NAD^+ and methanol present were at minimum three times higher. Controls with no enzymes did not show any activity.

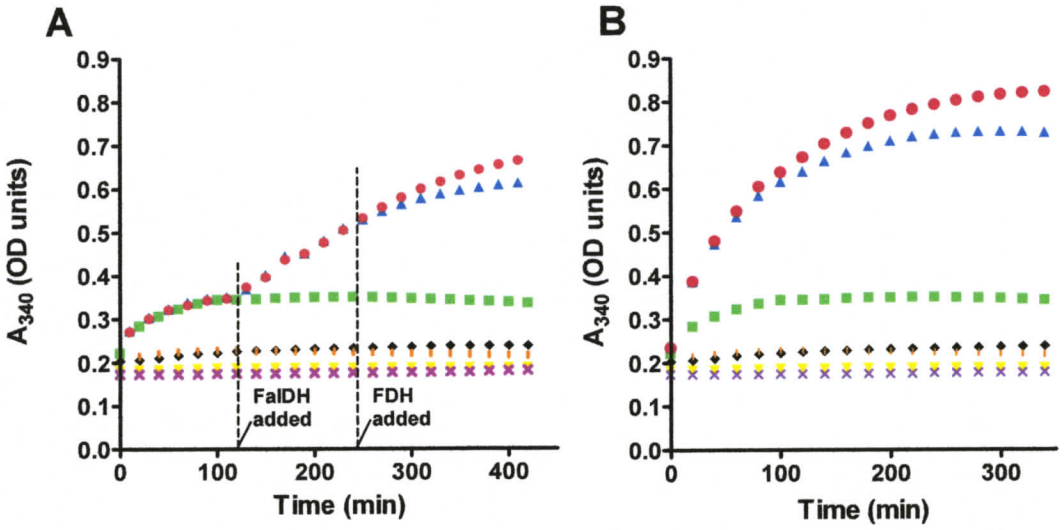

Figure 5.2 Multienzyme sequential and simultaneous oxidation of methanol to CO_2. A) Oxidation of methanol by adding enzymes in sequence. Reaction begins with ADH present, and the additions of FalDH and FDH are indicated. Progress curves are indicated by: ● = ADH, then FalDH, then FDH, ▲ = ADH, then FalDH, ■ = ADH only. B) Oxidation of MeOH by enzymes present simultaneously. ● = ADH + FalDH + FDH ▲ = ADH + FalDH, ■ = ADH only. Control trials in both A and B are indicated by: ◆ = Enzymes + NAD^+, no MeOH, ▮ = ADH + MeOH, no NAD^+, ▼ = ADH, no MeOH, no NAD^+, × = no enzyme control. [NAD^+] = 1 mM. Enzyme ratios used in these tests were 1.5 U ADH : 1 U FalDH : 0.1 U FDH. Reactions were performed at 25°C.

Neither the stepwise nor the simultaneous multi-enzyme trials had high NAD^+ utilization. Based on the NADH standard curve results, the master enzyme ratio of 1.5 U ADH: 1 U FalDH : 0.1 U FDH converted only 12% of the NAD^+ present into NADH.

Manipulation of the enzyme ratios could not much improve the results of the multienzyme trials. For example, adding 10 times more FDH to the system increased the yield to only 13%. Increasing the amount of ADH in the system was found to be most effective; doubling the amount of ADH while keeping the other enzyme concentrations the same increased NAD^+ utilization to 16%. By comparison, the same amount of FDH used in these assays (with a concentration of 0.1 M formate) can convert 100% of the NAD^+ to NADH. As well, the amount of FalDH used in these tests is enough to consume 83% of the NAD^+ present, using 0.1 M formaldehyde. ADH in isolation from the other enzymes can convert only 2% of the NAD^+ to NADH in the presence of 0.1 M methanol.

The results for the modified enzyme ratio tests are shown in Table 5. Notably, FalDH in isolation from the other enzymes produced a small but reproducible increase in absorption when incubated with NAD^+; this effect increased slightly when methanol was also included. An activity comparison of each of the three enzymes individually immobilized in gel is shown in Figure 5.3. Each enzyme was tested in a polyacrylamide gel cylinder setup with its respective C_1 substrate over two hours. The progress curves shown in Figure 5.3 were obtained by subtracting the no-substrate control curves from the enzyme-substrate-NAD^+ curves. FDH GAV is the only enzyme of the three to retain significant amounts of activity.

Table 5: Characterization of the solvated MLDP using various enzyme ratios

Substrate	[NAD^+]	ADH	FalDH	FDH	Initial Activity (mOD/min)	% NAD^+ Utilization (over 1 h)
Formate	1 mM	-	-	1x	191.9	100%
Formate	-	-	-	1x	0	0%
Formaldehyde	1 mM	-	1x	-	234.2	82%
Formaldehyde	-	-	1x	-	0	0%
Formaldehyde	1 mM	-	1x	1x	231.5	85%
Methanol	1 mM	1x	-	-	8.3	2%
Methanol	1 mM	1x	-	1x	8.0	2%
Methanol	1 mM	-	1x	1x	0.11	0.3%
Methanol	1 mM	1x	1x	-	24.9	12%
Methanol	1 mM	1x	1/2x	-	23.4	11.4%
Methanol	1 mM	1x	1/3x	-	25.8	11.8%
Methanol	1 mM	1x	2x	-	24.6	12%
Methanol	1 mM	1x	1x	1x	24.3	12%
Methanol	1 mM	2x	1x	1x	34.9	16%
Methanol	1 mM	1x	2x	1x	23.2	12%
Methanol	1 mM	1x	1x	2x	22.7	12%
Methanol	1 mM	-	-	1x	0	0%
Methanol	1 mM	-	-	-	0	0%
Methanol	-	1x	-	-	1.6	0.8%
Methanol	-	-	1x	-	0	0%
Methanol	-	-	-	1x	0	0%
Methanol	1 mM	-	1x	-	0.73	1.6%
-	1 mM	-	1x	-	0.48	1.1%
-	1 mM	1x	1x	1x	0.50	1%
-	1 mM	1x	-	-	0.96	0.8%
-	1 mM	-	-	-	0	0%

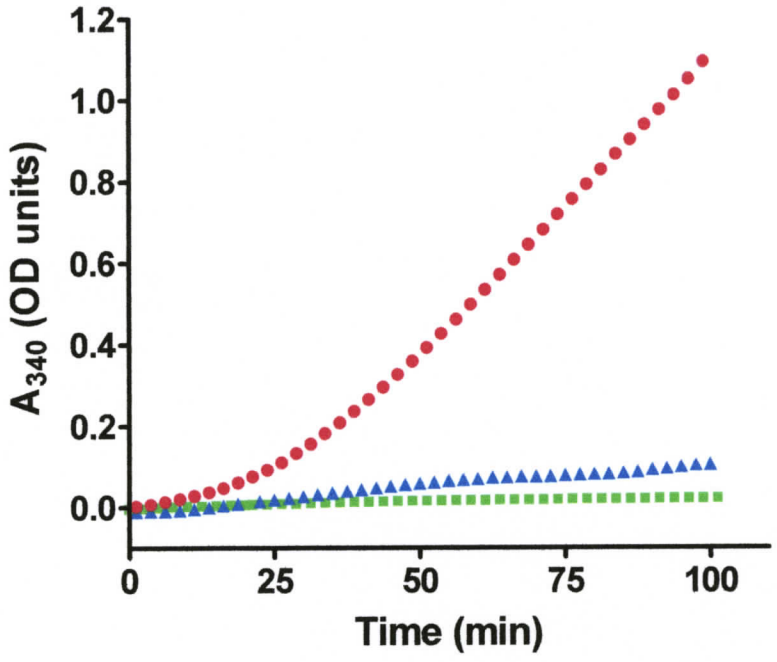

Figure 5.3 Activities of polyacrylamide-immobilized ADH, FalDH, and FDH. ● = Immobilized FDH with 0.1 M formate, ▲ = Immobilized FalDH with 0.1 M formaldehyde, ■ = Immobilized ADH with 0.1 M methanol. Traces were corrected by subtraction of no-substrate controls (N=2). [NAD^+] = 1 mM. Enzyme ratios used in these tests were: 1.5 U ADH:1 U FalDH:0.1 U FDH. Reactions were performed at 25°C.

Using 0.1 M formate, approximately 51% of the NAD^+ was converted to NADH over the two hour time period, whereas FalDH and ADH incubated with similar amounts of the appropriate substrates converted only 3% and 1%, respectively. The no-substrate controls for both FDH and ADH did not show much of an increase in absorbance. As a result, these corrected progress curves look nearly identical to the original uncorrected curves. Unlike the no-substrate controls for immobilized ADH and FDH, immobilized FalDH showed a reproducible and relatively large increase in absorbance in the absence of formaldehyde, equivalent to 8.7% of the NAD^+ being converted. Consequently, the absorbance increase of any immobilized multienzyme trial that contained both FalDH and NAD^+ can be attributed largely to this effect. In fact, progress curves of trials with all three enzymes incubated with 0.1 M methanol were almost identical to ones with only NAD^+ and FalDH present. Aqueous solutions of FalDH incubated with only NAD^+ did show small increases in absorbance (equivalent to an NAD^+ conversion of approximately 1%), but these activity levels were close to the lower detection limit of the microplate reader. When compared with FalDH in aqueous solution, the immobilized FalDH showed approximately 16 times higher initial ΔA_{340} when incubated with NAD^+ alone.

5.4) Discussion

5.4.1) Characterization of the solvated multienzyme system

Based on the results obtained for the solvated multienzyme trials, the three selected dehydrogenases are compatible with each other. The stepwise addition of enzymes shows an increase in activity with the addition of each subsequent enzyme,

suggesting each enzyme is contributing to the reaction. It should be noted that the manufacturer of the horse liver ADH states that some NAD^+ is present in the enzyme preparation. This would explain the slight increases in absorbance observed in the no-NAD^+ controls.

It is difficult to determine the relative contribution of each enzyme in the three-enzyme case, but based on the data, it seems that adding FalDH to ADH has more of an effect than adding FDH to the first two enzymes. There is some evidence that the interaction of formaldehyde with horse liver ADH influences the maximal rate of methanol dehydrogenation, so some product inhibition may be occurring (Mani *et al.*, 1970). If this is the case, then the presence of FalDH could alleviate it and contribute to the higher reaction rate. Another possibility is that side reactions are occurring. When formaldehyde is solvated in water in the presence of methanol, they can react to form formaldehyde-methyl-hemiacetal. This can undergo a further reaction via the dismutase activity of horse liver ADH to form methyl formate (Abeles and Lee, 1960). This is a dead-end pathway with respect to NADH production, as FDH cannot act upon methyl formate (Egorov *et al.*, 1979). Complicating matters further is the fact that FalDH itself has dismutase activity, which would convert some of the formaldehyde back into methanol instead of forward to formate (Oppenheimer *et al.*, 1996). When FalDH and FDH were incubated with 0.1 M formaldehyde, these trials only marginally improved the NAD^+ conversion over one hour as compared to the FalDH only case, suggesting the system is indeed not simply just a one-way chain.

Speaking purely from a comparison of individual relative activities under substrate-saturated conditions, one might predict that the performance of a multienzyme chain based on these dehydrogenases might be limited by ADH. Based on the results of the variable enzyme ratio tests, this seems to be an accurate prediction. Trials containing ADH and FalDH were also informative; increasing the amount of FalDH did not increase the yield of NADH, and decreasing it did not cause the yield to drop more than 1%. This could suggest that a large amount of the FalDH added is not participating in the reaction, likely because there is not a lot of formaldehyde present in the system at any particular moment.

5.4.2) Characterization of the immobilized multienzyme system

Judging from the results of the immobilized multienzyme trials, polyacrylamide is not a suitable immobilization agent for ADH and FalDH. The corrected progress curve of immobilized ADH is essentially flat, and that of FalDH is much the same. The most obvious explanation is that the acrylamide is interfering with these enzymes also. Preliminary activity tests on ADH and FalDH after incubation with 12.5% acrylamide for one minute suggest that this is indeed the case. While FDH retained 36% of its activity after the same treatment, FalDH and ADH displayed essentially no activity at all. Although a full analysis of the acrylamide effect on these two enzymes was not performed, this is interesting in light of the fact that FDH has had its acrylamide-reactive surface cysteines replaced by bioengineering, while ADH and FalDH have not.

The most intriguing aspect of these assays was the unexpected and dramatic increase in absorbance for any trial containing both immobilized FalDH and NAD^+. The presence of substrate in the form of either methanol or formaldehyde did not seem to affect either the maximum reaction velocity or the OD attained after one hour, which suggests there is another reducing agent involved. It is unclear what the reducing agent in this FalDH-NAD^+ reaction would be, as there were no other species present in the analyte. To investigate this matter further, it would be instructive to include an inhibitor of FalDH to determine if the increase in absorbance is indeed due to a catalytic conversion of NAD^+ to NADH by FalDH. A chelating agent such as *o*-phenanthroline or a heavy metal such as Ni or Cd should be suitable for this purpose (Ando *et al.*, 1979; Ogushi *et al.*, 1984). If this increase in absorbance remains unchanged in the presence of inhibitor, then this would strongly suggest a non-catalytic origin for this effect.

It should be noted that when FalDH is behaving as a dismutase in the cell, the nicotinamide cofactor is bound tightly within the active site and is not exchanged with the cofactor pool in the cytosolic medium (Tanaka *et al.*, 2002). Thus, it is possible that there is in fact a source of NADH within FalDH itself. If immobilization in acrylamide destabilizes the structure of FalDH, this could dislodge the tightly bound cofactor. However, this would produce at most four molecules of NADH per molecule of FalDH, resulting in a nanomolar-scale increase in NADH. If the unexpected increase in absorbance is indeed due to NADH entering the analyte, this is several orders of magnitude too small to be a satisfactory explanation. Investigations into this effect are ongoing.

5.4.3) Final evaluation of the MLDP system

Based on the results obtained in this study, the power density of the biofuel cell constructed by Whitesides *et al.* could be improved via manipulation of the enzyme ratios. This fuel cell used a ratio of approximately 0.3 U ADH : 1 U FalDH : 0.1 U FDH. Since this ratio did not show activity levels that were high enough to measure accurately, the proportion of ADH was increased for this study to give 1.5 U ADH : 1 U FalDH : 0.1 U FDH. However, as seen in the results, additional increases of the ADH concentration were found to improve the activity even more. It could be that the ideal enzyme ratio for these three enzymes cannot be economically achieved; at some point, further increases in the concentration of ADH will likely become cost-limiting.

Ultimately, it seems that horse liver ADH must be replaced with another enzyme. Unfortunately, most methanol-oxidizing enzymes in bacteria appear to be quinoprotein dependent as opposed to NAD^+- dependent. As such, they are not as suitable to be integrated into this system. NAD^+- dependent methanol dehydrogenase from *Bacillus methanolicus* has already been mentioned as a potential candidate, but it has problems of its own, such as poor stability. The ADH from *Bacillus stearothermophilus* 2334 is an attractive possibility from the standpoint of its kinetic parameters; it has a k_{cat} / K_m value nearly twice that of horse liver ADH (Sheehan *et al.*, 1988). This protein has been expressed in *E. coli* (Dowds et al., 1988), but it is not currently available as a commercial preparation. If a suitable ADH cannot be found or cannot be produced economically, it may be desirable to bioengineer a known ADH enzyme. For example, directed evolution

could be performed to expand the substrate specificity of yeast ADH from ethanol to include methanol also.

Further characterization of the MLDP system would involve measurement of the steady state reaction constants for each enzymatic reaction in the system. If these parameters are measured accurately, the algebraic rate equations for the individual reactions can be combined and inputted into equation-solving software such as Maple or Mathematica to obtain a realistic model of the system (Stoner, 1993). For example, experimental data from a three-enzyme system of creatine kinase, hexokinase, and glucose 6-phosphate dehydrogenase closely matched predictions obtained from a mathematical model (Yildirim *et al.*, 2002). As well, mathematical models that account for diffusional effects and product inhibition have been created for immobilized enzyme systems (Rees, 1984). If the MLDP system is to eventually become applicable to industry, this type of analysis would maximize the chances of success.

Chapter 6 : Summary and Conclusions

"Every honest researcher I know admits he's just a professional amateur. He's doing whatever he's doing for the first time. That makes him an amateur. He also has sense enough to know that he's going to have a lot of trouble. That makes him a professional."

-- Charles Franklin Kettering (1876 – 1958), U.S. engineer and inventor.

The expression and purification of *Myc*FDH in this study was successful in that a high degree of purity was obtained. The main challenge associated with these tests was the low degree of soluble protein expression. Various efforts to improve the solubility of the protein were unsuccessful, so it may be concluded that the pET system is not an ideal expression vector for this protein if maximization of the protein yield is desired. Based on the results of the different tag variants of this protein, it seems that including a hexahistidine tag at the C-terminal end of the protein is less effective than tagging at the N-terminus, possibly due to post-translational modification of the C-terminal region of the protein.

The purification experiments in this work were limited to the trial scale, but nevertheless some inferences may be made about the feasibility of scaling up this process. A packed-column type setup would likely increase the amount of FDH retained on the gel, due to a higher resin : enzyme ratio and longer overall binding time. As seen in this study, ammonium sulfate precipitation is an effective means of concentrating the

protein, and so the larger lysate volumes associated with scaling up could easily be accommodated with this technique. However, it is unlikely that a commercial purification regime based on affinity chromatography could compete economically with the production of FDH GAV, and so it seems that further studies on the MLDP system should be focused on finding a suitable replacement for the first enzyme in the chain, ADH. A possible replacement is ADH 2334 from *Bacillus stearothermophilus*, which displays methanol activity with kinetic parameters that are more attractive than those of horse liver alcohol dehydrogenase. Commercial preparations of this protein could most likely be produced cheaply, as the protein is expressible in *E. coli*. An improved version of the MLDP, once optimized for enzyme ratios, would undoubtedly produce higher current densities and open cell voltages than those obtained in the previous study.

The reversibility of the acrylamide monomer inhibition and the identical K_m values for both aqueous and immobilized FDH GAV suggest that polyacrylamide is a non-disruptive immobilization agent for this protein. The same cannot be said for FalDH and ADH, however. Thus, a new type of matrix must be investigated if an immobilized version of the MLDP is to be of any use. Both ADH and FDH retain over 50% of their activity when immobilized in glyoxal agarose (Bolivar *et al.*, 2006a; Bolivar *et al.*, 2006b), which makes this matrix an obvious first choice for further research into immobilized versions of this multienzyme system.

Perhaps the most successful aspect of this work was the development of a high-throughput method to determine the *in situ* activity of gel-immobilized enzymes. If the

CPIDER setup could be improved to create gel cylinders with walls a few tens of microns thick, this could have implications for microchannel flow cell technologies. The fact that polyacrylamide gel can be cast into any desired shape makes it especially suited to microfabrication techniques such as those used in the development of microscale fuel cells. Using long, convoluted microcapillaries surrounded by a thin layer of enzyme-gel matrix would maximize the surface area to volume ratio of the setup, which promotes efficient use of the substrate. As well, the flow stream in these capillaries is laminar and behaves in a highly predictable manner (Miyazaki and Maeda, 2006).

Synthetic organic chemistry is often viewed as an art form; many factors such as chirality, side reactions, and undesired byproducts must be taken into account. Over the past 30 years, enzymes have revolutionized this art form by replacing traditional inorganic catalysts in over 100 industrial processes (Straathof *et al.*, 2002), and many more are in development. The basic strategy in many bioengineering efforts is to make individual point mutants to determine which residues to target for replacement, and then determine which residues are most appropriate as replacements. Favorable mutations can then be combined into one multiple-mutant variant of the protein. Given that this is a time-intensive process, it is not surprising that the optimization of FDH GAV required three decades. FDH GAV is an atypical example, however; most proteins used in industry are not altered nearly as heavily. Sometimes, as in the case of *Myc*FDH, replacing only a few surface cysteine residues is sufficient to stabilize the protein against harsh organics present in the reaction mixture (Yamamoto *et al.*, 2004). With the advent

of more powerful protein modeling software and directed evolution techniques, tailor-made "designer proteins" may be realized within this generation.

Bibliography

Abeles, R. H. and Lee, H. A. (1960). The dismutation of formaldehyde by liver alcohol dehydrogenase. *The Journal of Biological Chemistry* **235**, 1499-1503.

Akers, N. L., Moore, C. M. and Minteer, S. D. (2004). Development of alcohol / O_2 biofuel cells using salt-extracted tetrabutylammonium bromide / Nafion membranes to immobilize dehydrogenase enzymes. *Electrochimica Acta* **50**, 2521-2525.

Ando, M., Yoshimoto, T., Ogushi, S., Rikitake, K., Shibata, S. and Tsuru, D. (1979). Formaldehyde dehydrogenase from *Pseudomonas putida*: Purification and some properties. *Journal of Biochemistry* **85**, 1165-1172.

Ansorge-Schumacher, M. B., Slusarczyk, H., Schümers, J. and Hirtz, D. (2006). Directed evolution of formate dehydrogenase from *Candida boidinii* for improved stability during entrapment in polyacrylamide. *FEBS Journal* **273**, 3938-3945.

Baneyx, F. (1999). Recombinant protein expression in *Escherichia coli*. *Current Opinion in Biotechnology* **10**, 411-421.

Baneyx, F. and Mujacic, M. (2004). Recombinant protein folding and misfolding in *Escherichia coli*. *Nature Biotechnology* **22**, 1399-1408.

Barrière, F., Kavanagh, P. and Leech, M. (2006). A laccase-glucose oxidase biofuel cell prototype operating in a physiological buffer. *Electrochimica Acta* **51**, 5187-5192.

Bolivar, J. M., Wilson, L., Ferrarotti, S. A., Fernández-Lafuente, R., Guisán, J. M. and Mateo, C. (2006a). Stabilization of a formate dehydrogenase by covalent immobilization on highly activated glyoxyl-agarose supports. *Biomacromolecules* **7**, 669-673.

Bolivar, J. M., Wilson, L., Ferrarotti, S. A., Guisán, J. M., Fernández-Lafuente, R. and Mateo, C. (2006b). Improvement of the stability of alcohol dehydrogenase by covalent immobilization on glyoxyl-agarose. *Journal of Biotechnology* **125**, 85-94.

Bordini, E., Hamdan, M. and Righetti, P. G. (2000). Probing acrylamide alkylation sites in cysteine-free proteins by matrix-assisted laser desorption/ionization time-of-flight. *Rapid Communications in Mass Spectrometry* **14**, 840-848.

Braidwood, R. J., Sauer, J. D., Helbaek, H., Mangelsdorf, P. C., Cutler, H. C., Coon, C. S., Linton, R., Steward, J. and Oppenheim, A. L. (1953). Symposium: Did man once live by beer alone? *American Anthropologist* **55**, 515-526.

Bray, G. A., Nielsen, S. J. and Popkin, B. M. (2004). Consumption of high-fructose corn syrup in beverages may play a role in the epidemic of obesity. *American Journal of Clinical Nutrition* **79**, 537-543.

Buchholz, K., Kasche, V. and Bornscheuer, U. T. (2005). Introduction to enzyme technology. In *Biocatalysts and Enzyme Technology*. Weinheim: Wiley - VCH Verlag GmbH & Co.

Buchner, E. (1897). Alkoholische gährung ohne hefezellen. *Berichte der Deutschen Chemischen Gesellschaft* **30**, 117-124.

Bullen, R. A., Arnot, T. C., Lakeman, J. B. and Walsh, F. C. (2006). Biofuel cells and their development. *Biosensors and Bioelectronics* **21**, 2015-2045.

Chaga, G. S. (2001). Twenty-five years of immobilized metal ion affinity chromatography: Past, present and future. *Journal of Biochemical and Biophysical Methods* **49**, 313-334.

Chauhan, G. S., Chauhan, S., Kumar, Y., Thakur, U. S., Kanwar, S. S. and Kaushal, R. (2006). Designing acrylamide- and methylacrylate-based novel supports for lipase immobilization. *Journal of Applied Polymer Science* **105**, 3006-3016.

Chen, A. K. and Liu, C. C. (1977). Electrochemical evaluation of lactate dehydrogenase immobilized in polyacrylamide gels. *Biotechnology and Bioengineering* **19**, 1785-1792.

Chiari, M., Righetti, P. G., Negri, A., Ceciliani, F. and Ronchi, S. (1992). Preincubation with cysteine prevents modification of sulfhydryl groups in proteins by unreacted acrylamide in a gel. *Electrophoresis* **13**, 882-884.

Cohen, B. (1931). The bacterial culture as an electrical half-cell. *Journal of Bacteriology* **21**, 18-19.

Davis, F. and Higson, S. P. J. (2007). Biofuel cells - Recent advances and applications. *Biosensors and Bioelectronics* **22**, 1224-1235.

Dickson, R. M., Norris, D. J., Tzeng, Y. and Moerner, W. E. (1996). Three-dimensional imaging of single molecules solvated in pores of poly(acrylamide) gels. *Science* **274**, 966-969.

Dixon, M. (1951). Multi-enzyme systems. London: Cambridge University Press.

Dixon, M. and Webb, E. C. (1964). Enzymes. New York: Academic Press.

Dowds, B. C. A., Sheehan, M. C., Bailey, C. J. and McConnell, D. J. (1988). Cloning and characterization of the gene for a methanol-utilizing alcohol dehydrogenase from *Bacillus stearothermophilus*. *Gene* **68**, 11-22.

Drozdov-Tikhomirov, L. N. and Dorodnov, A. V. (1992). Optimal structure of a multi-enzyme system. *Molekularnaya Biologiya* **25**, 1382-1390.

Egorov, A. M., Avilova, T. V., Dikov, M. M., Popov, V. O., Rodionov, Y. V. and Berezin, I. V. (1979). NAD-dependent formate dehydrogenase from methylotrophic bacterium, Strain 1: Purification and characterization. *European Journal of Biochemistry* **99**, 569-576.

Galkin, A., Kulakova, L., Tishkov, V. I., Esaki, N. and Soda, K. (1995). Cloning of formate dehydrogenase gene from a methanol utilizing bacterium *Mycobacterium vaccae* N10. *Applied Microbiology and Biotechnology* **44**, 479-483.

Galkin, A. G., Kutsenko, A. S., Bajulina, N. P., Esipova, N. G., Lamzin, V. S., Mesentzev, A. V., Shelukho, D. V., Tikhonova, T. V., Tishkov, V. I., Ustinnikova, T. B. and Popov, V. O. (2001). Site-directed mutagenesis of the essential arginine of the formate dehydrogenase active centre. *Biochimica et Biophysica Acta* **1594**, 136-149.

Gonzáles-Sáiz, J. M. and Pizarro, C. (2001). Polyacrylamide gels as support for enzyme immobilization by entrapment. Effect of polyelectrolyte carrier, pH and temperature on enzyme action and kinetics parameters. *European Polymer Journal* **37**, 435-444.

Gorrebeeck, C., Spanoghe, M., Lanens, D., Lemière, G. L., Dommisse, R. A., Lepoivre, J. A. and Alderweireldt, F. C. (1991). Permeability studies on horse liver alcohol dehydrogenase (HLAD) in polyacrylamide gel beads. *Recueil de Travaux Chimiques des Pays-Bas* **110**, 231-235.

Hamilton, B. K., Gardner, C. R. and Colton, C. K. (1974). Effect of diffusional limitations on Lineweaver-Burk plots for immobilized enzymes. *American Institute of Chemical Engineers Journal* **20**, 503-510.

Hammarström, M., Hellgren, N., van den Berg, S., Berglund, H. and Härd, T. (2002). Rapid screening for improved solubility of small human proteins produced as fusion proteins in *Escherichia coli*. *Protein Science* **11**, 313-321.

Hektor, H. J., Kloosterman, H. and Dijkhuizen, L. (2002). Identification of a magnesium-dependent NAD(P)(H)-binding domain in the nicotinoprotein methanol dehydrogenase from *Bacillus methanolicus*. *Journal of Biological Chemistry* **277**, 46966-46973.

Hirel, P. H., Schmitter, M. J., Dessen, P., Fayat, G. and Blanquet, S. (1989). Extent of N-terminal methionine excision from *Escherichia coli* proteins is governed by the side-chain length of the penultimate amino acid. *Proceedings of the National Academy of Sciences USA* **86**, 8247-8251.

Holmes, D. L. and Stellwagen, N. C. (1991). Estimation of polyacrylamide gel pore size from Ferguson plots of linear DNA fragments II. Comparison of gels with

different crosslinker concentrations, added agarose and added linear polyacrylamide. *Electrophoresis* **12**, 612-619.

Ito, K., Takahashi, M., Yoshimoto, T. and Tsuru, D. (1994). Cloning and high-level expression of the glutathione-independent formaldehyde dehydrogenase gene from *Pseudomonas putida*. *Journal of Bacteriology* **176**, 2483-2491.

Iwami, K., Wang, J. Y., Jain, R., McCormack, S. and Johnson, L. R. (1990). Intestinal ornithine decarboxylase: half-life and regulation by putrescine. *American Journal of Physiology - Gastrointestinal and Liver Physiology* **258**, G308-G315.

Jansen, K., Thauer, R. K., Widdel, F. and Fuchs, G. (1984). Carbon assimilation pathways in sulfate reducing bacteria. Formate, carbon dioxide, carbon monoxide, and acetate assimilation by *Desulfovibrio baarsii*. *Archives of Microbiology* **138**, 257-262.

Kajiwara, S. and Maeda, H. (1986). Co-immobilization of malate dehydrogenase and formate dehydrogenase in polyethyleneglycol (#4000)diacrylate gel by droplet gel-entrapping method. *Biotechnology and Bioengineering* **28**, 1794-1800.

Kajiwara, S. and Maeda, H. (1987). The improvement of a droplet gel-entrapping method: The co-immobilization of leucine dehydrogenase and formate dehydrogenase. *Agricultural and Biological Chemistry* **51**, 2873-2879.

Katz, E., Willner, I. and Kotlyar, A. B. (1999). A non-compartmentalized glucose / O_2 biofuel cell by bioengineered electrode surfaces. *Journal of Electroanalytical Chemistry* **479**, 64-68.

Kiianitsa, K., Solinger, J. A. and Heyer, W. (2003). NADH-coupled microplate photometric assay for kinetic studies of ATP-hydrolyzing enzymes with low and high specific activities. *Analytical Biochemistry* **321**, 266-271.

Kjeang, E., Sinton, D. and Harrington, D. A. (2006). Strategic enzyme patterning for microfluidic biofuel cells. *Journal of Power Sources* **158**, 1-12.

Klibanov, A. M. (1983). Immobilized Enzymes and Cells as Practical Catalysts. *Science* **219**, 722-727.

Klyachko, N. L., Vakula, S. V., Gladyshev, V. N., Tishkov, V. I. and Levashov, A. V. (1997). Formate dehydrogenase in a reversed micelle system: Regulation of catalytic activity and oligomeric composition of the enzyme. *Biochemistry (Moscow)* **62**, 1439-1443.

Knight, P. (1990). Bioseparations - Media and methods. *Bio-technology* **8**, 200-201.

Kragl, U., Vasic-Racki, D. and Wandrey, C. (1996). Continuous production of L-*tert*-leucine in series of two enzyme membrane reactors. *Bioprocess Engineering* **14**, 291-297.

Kutzenko, A. S., Lamzin, V. S. and Popov, V. O. (1998). Conserved supersecondary structural motif in NAD-dependent dehydrogenases. *Federation of European Biochemical Societies Letters* **423**, 105-109.

Lamzin, V. S., Dauter, Z., Popov, V. O., Harutyunyan, E. H. and Wilson, K. S. (1994). High resolution structures of holo and apo formate dehydrogenase. *Journal of Molecular Biology* **236**, 759-785.

Liu, S. and Ju, H. (2003). Reagentless glucose biosensor based on direct electron transfer of glucose oxidase on colloidal gold modified carbon paste electrode. *Biosensors and Bioelectronics* **19**, 177-183.

Mani, J., Pietruszko, R. and H., T. (1970). Methanol activity of alcohol dehydrogenases from human liver, horse liver, and yeast. *Archives of Biochemistry and Biophysics* **140**, 52-59.

Marx, C. J., Miller, J. A., L., C. and Lidstrom, M. E. (2004). Multiple formaldehyde oxidation / detoxification pathways in *Burkholderia fungorum* LB400. *Journal of Bacteriology* **186**, 2173-2178.

Missiakas, D., Schwager, F., Betton, J. M., Georgopoulos, C. and Raina, S. (1996). Identification and characterization of HslV HslU (ClpQ ClpY) proteins involved in overall proteolysis of misfolded proteins in *Escherichia coli*. *European Molecular Biology Organization Journal* **15**, 6899-6909.

Mitchell, P. (1979). Keilin's respiratory chain concept and its chemiosmotic consequences. *Science* **206**, 1148-1159.

Miyazaki, M. and Maeda, H. (2006). Microchannel enzyme reactors and their applications for processing. *Trends in Biotechnology* **24**, 463-470.

Mosbach, K. and Mosbach, R. (1966). Entrapment of enzymes and microorganisms in synthetic cross-linked polymers and their application in column techniques. *Acta Chemica Scandinavia* **20**, 2807-2810.

Mukhopadhyay, A. (1997). Inclusion bodies and purification of proteins in biologically active forms. *Advances in Biochemical Engineering and Biotechnology* **56**, 61-109.

Nilsson, H., Mosbach, R. and Mosbach, K. (1972). The use of bead polymerization of acrylic monomers for immobilization of enzymes. *Biochimica et Biophysica Acta* **268**, 253-256.

Ogushi, S., Ando, M. and Tsuru, D. (1984). Formaldehyde dehydrogenase from *Pseudomonas putida*: A zinc metalloenzyme. *Journal of Biochemistry* **96**, 1587-1591.

Ohshima, T., Wandrey, C., Kula, M. and Soda, K. (1985). Improvement for L-Leucine production in a continuously operated enzyme membrane reactor. *Biotechnology and Bioengineering* **27**, 1616-1618.

Oppenheimer, N. J., Henehan, G. T. M., Huete-Pérez, J. A. and Ito, K. (1996). *P. putida* formaldehyde dehydrogenase: An alcohol dehydrogenase masquerading as an aldehyde dehydrogenase. In *Enzymology and Molecular Biology of Carbonyl Metabolism*, vol. 6 (ed. H. Weiner). New York: Plenum Press.

Palmore, G. T. R., Bertschy, H., Bergens, S. H. and Whitesides, G. M. (1998). A methanol / dioxygen biofuel cell that uses NAD^+- dependent dehydrogenases as catalysts: application of an electro-enzymatic method to regenerate nicotinamide adenine dinucleotide at low overpotentials. *Journal of Electroanalytical Chemistry* **443**, 155-161.

Peimbert, M. and Segovia, L. (2003). Evolutionary engineering of a beta-lactamase activity on a D-Ala D-Ala transpeptidase fold. *Protein Engineering* **16**, 27-35.

Pizarro, C., Fernández-Torroba, M. A., Benito, C. and Gonzáles-Sáiz, J. M. (1996). Optimization by experimental design of polyacrylamide gel composition as support for enzyme immobilization by entrapment *Biotechnology and Bioengineering* **53**, 497-506.

Pluschkell, S. B. and Flickinger, M. C. (2002). Dissimilation of [^{13}C] methanol by continuous cultures of Bacillus methanolicus MGA3 at 50°C studied by ^{13}C NMR and isotope-ratio mass spectrometry. *Microbiology* **148**, 3223-3233.

Popov, V. O. and Egorov, A. M. (1979). Essential SH-groups of bacterial formate dehydrogenase. *Biochemistry (Moscow)* **2**, 161-166.

Popov, V. O. and Lamzin, V. S. (1994). NAD^+-dependent formate dehydrogenase. *Biochemical Journal* **301**, 625-643.

Popov, V. O. and Rodionov, Y. V. (1978). NAD-dependent formate dehydrogenase from methylotrophic bacteria - Study of kinetic mechanism. *Bioorganicheskaya Khimiya* **4**, 117-128.

Popov, V. O. and Tishkov, V. I. (2003). NAD^+-dependent formate dehydrogenase. From a model enzyme to a versatile biocatalyst. In *Protein Structures: Kaleidoscope of Structural Properties and Functions*, (ed. V. N. Uversky). Kerala, India: Research Signpost.

Porath, J., Carlsson, J., Olsson, I. and Belfrage, G. (1975). Metal chelate affinity chromatography, a new approach to protein fractionation. *Nature* **258**, 598-599.

Rees, D. C. (1984). A general solution for the steady-state kinetics of immobilized enzyme systems. *Bulletin of Mathematical Biology* **46**, 229-234.

Ribbons, D. W., Harrison, J. E. and Wadzinski, A. M. (1970). Metabolism of single carbon compounds. *Annual Reviews of Microbiology* **24**, 135-158.

Rodionov, Y. V., Avilova, T. V. and Popov, V. O. (1977). NAD-dependent formate dehydrogenase from methylotrophic bacteria: Study of the properties and stability of soluble and immobilized enzymes. *Biokhimiya* **42**, 2020-2026.

Rodionov, Y. V., Avilova, T. V., Zakharova, E. V., Platonenkova, L. S., Egorov, A. M. and Berezin, I. V. (1978). Purification and basic properties of NAD-dependent formate dehydrogenase from methylotrophic bacteria. *Biokhimiya* **42**, 1896-1904.

Rojkova, A. M., Galkin, A. G., Kulakova, L. B., Serov, A. E., Savitsky, P. A., Fedorchuk, V. V. and Tishkov, V. I. (1999). Bacterial formate dehydrogenase: Increasing the enzyme thermal stability by hydrophobization of alpha-helices. *FEBS Letters* **445**, 183-188.

Seelig, B. and Szostak, J. W. (2007). Selection and evolution of enzymes from a partially randomized non-catalytic scaffold. *Nature* **448**, 828-833.

Shaked, Z. and Whitesides, G. M. (1980). Enzyme-catalyzed organic synthesis: NADH regeneration by using formate dehydrogenase. *Journal of the American Chemical Society* **102**, 7104-7105.

Sheehan, M. C., Bailey, C. J., Dowds, B. C. A. and McConnell, D. J. (1988). A new alcohol dehydrogenase, reactive towards methanol, from *Bacillus stearothermophilus*. *Biochemical Journal* **252**, 661-666.

Sheehan, T. G. and Tully, E. R. (1983). Purine biosynthesis *de novo* in rat skeletal muscle. *Biochemical Journal* **216**, 605-610.

Sheldon, R. A. (2007). Enzyme Immobilization: The Quest for Optimum Performance. *Advances in Synthesis and Catalysis* **349**, 1289-1307.

Soukharev, V., Mano, N. and Heller, A. (2004). A four-electron O_2-electroreduction biocatalyst superior to platinum and a biofuel cell operating at 0.88 V. *Journal of the American Chemical Society* **126**, 8368-8369.

Srere, P. A., Mattiasson, B. and Mosbach, K. (1973). An immobilized three-enzyme system: A model for microenvironmental compartmentalization in mitochondria. *Proceedings of the National Academy of Sciences USA* **70**, 2534-2538.

Stoner, C. D. (1993). Quantitative determination of the steady-state kinetics of multienzyme reactions using the algebraic rate equations for the component single-enzyme reactions. *Biochemical Journal* **291**, 585-593.

Straathof, A. J. J., Panke, S. and Schmid, A. (2002). The production of fine chemicals by biotransformation. *Current Opinion in Biotechnology* **13**, 548-556.

Studier, F. W. and Moffatt, B. A. (1986). Use of bacteriophage T7 RNA polymerase to direct selective high-level expression of cloned genes. *Journal of Molecular Biology* **189**, 113-130.

Subramanian, S. (1984). Dye-ligand affinity chromatography: The interaction of Cibacron Blue F3GA with proteins and enzymes. *CRC Critical Reviews in Biochemistry* **16**, 169-205.

Tanaka, N., Kusakabe, Y., Ito, K., Yoshimoto, T. and Nakamura, K. T. (2002). Crystal structure of formaldehyde dehydrogenase from *Pseudomonas putida*: The structural origin of the tightly bound cofactor in nicotinoprotein dehydrogenases. *Journal of Molecular Biology* **324**, 519-533.

Tauber, H. (1949). The chemistry and technology of enzymes. New York: Wiley.

Tischer, W. and Wedekind, F. (1999). Immobilized Enzymes: Methods and Applications. *Topics in Current Chemistry* **200**, 95-126.

Tishkov, V. I. and Egorov, A. M. (1985). Mechanism of the formate dehydrogenase reaction. *Biokhimiya* **50**, 1059-1066.

Tishkov, V. I., Galkin, A. and Egorov, A. M. (1990). NAD-dependent formate dehydrogenase of methylotrophic *Pseudomonas sp.* 101 bacteria: Cloning, expression, and study of the structure of the gene. *Doklady Akademii Nauk SSR* **317**, 745-748.

Tishkov, V. I., Galkin, A., Marchenko, G. N., Egorova, O. A., Sheluho, D. V., Kulakova, L., Dementieva, L. A. and Egorov, A. M. (1993). Catalytic properties and stability of a *Pseudomonas sp. 101* formate dehydrogenase mutants containing Cys-255-Ser and Cys-255-Met replacements. *Biochemical and Biophysical Research Communications* **192**, 976-981.

Tishkov, V. I., Matorin, A. D., Rojkova, A. M., Fedorchuk, V. V., Savitsky, P. A., Dementieva, L. A., Lamzin, V. S., Mezentzev, A. V. and Popov, V. O. (1996). Site-directed mutagenesis of the formate dehydrogenase active centre: Role of the His^{332}-Gln^{313} pair in enzyme catalysis. *FEBS Letters* **390**, 104-108.

Tishkov, V. I. and Popov, V. O. (2004). Catalytic mechanism and application of formate dehydrogenase. *Biochemistry (Moscow)* **69**, 1252-1267.

Tishkov, V. I. and Popov, V. O. (2006). Protein engineering of formate dehydrogenase. *Biomolecular Engineering* **23**, 89-110.

Tobias, J. W., Shrader, T. E., Rocap, G. and Varshavsky, A. (1991). The N-end rule in bacteria. *Science* **254**, 1374-1377.

Turner, P., Holst, O. and Karlsson, E. N. (2005). Optimized expression of soluble cyclomaltodextrinase of thermophilic origin in *Escherichia coli* by using a soluble fusion-tag and by tuning of inducer concentration. *Protein Expression and Purification* **39**, 54-60.

Wessel, T. (1984). The agricultural foundations of civilization. *Agriculture and Human Values* **1**, 9-12.

Wu, Y. and Hu, S. (2007). Biosensors based on direct electron transfer in redox proteins. *Microchimica Acta* **159**, 1-17.

Yamamoto, H., Mitsuhashi, K., Kimoto, N., Kobayashi, Y. and Esaki, N. (2005). Robust NADH-regenerator: Improved α-haloketone-resistant formate dehydrogenase. *Appl Microbiol Biotechnol* **67**, 33-39.

Yamamoto, H., Mitsuhashi, K., Kimoto, N., Matsuyama, A., Esaki, N. and Kobayashi, Y. (2004). A novel NADH-dependent carbonyl reductase from *Kluyveromyces aestuarii* and comparison of NADH-regeneration system for the synthesis of ethyl (*S*)-4-chloro-3-hydroxybutanoate. *Bioscience Biotechnology Biochemistry* **68**, 638-649.

Yan, M., Ge, J., Liu, Z. and Ouyang, P. (2006). Encapsulation of single enzyme in nanogel with enhanced biocatalytic activity and stability. *Journal of the American Chemical Society* **128**, 11008-11009.

Yildirim, N., Çiftçi, M. and Küfrevioğlu, O. I. (2002). Kinetic analysis of multi enzyme systems: A case study of the closed system of creatine kinase, hexokinase and glucose 6-phosphate dehydrogenase. *Journal of Mathematical Chemistry* **31**, 121-130.

Yurimoto, H., Kato, N. and Sakai, Y. (2005). Assimilation, dissimilation, and detoxification of formaldehyde, a central metabolic intermediate of methylotrophic metabolism. *The Chemical Record* **5**, 367-375.

Zadražil, A., Chmelíková, R. and Hasal, P. (2003). Continuous penicillin G hydrolysis in an electro-membrane reactor with immobilized penicillin G acylase. *Biotechnology Letters* **25**, 485-490.

Zhang, X., Ranta, A. and Halme, A. (2006). Direct methanol biocatalytic fuel cell - Considerations of restraints on electron transfer. *Biosensors and Bioelectronics* **21**, 2052-2057.